MASTER OF SCIENCE IN ELECTRICAL AND ELECTRONIC ENGINEERING

Design and analysis of a model predictive unified power flow controller (MPUPFC) for improving power system stability

Md. Shoaib Shahriar

Department of Electrical and Electronic Engineering
Islamic University of Technology
August 2012

Declaration of Candidate

It is hereby declared that this thesis/report or any part of it has not been submitted elsewhere for the award of any degree or diploma.

(Signature of the Supervisor)	(Signature of Candidate)
Prof. Dr. Md. Shahid Ullah	Md. Shoaib Shahriar
Designation: Professor	Student ID.:092615
Address: EEE Dept., IUT,	Academic Year: 2009-2010
Board Bazar, Gazipur-1704	

Dedicated to

My Beloved Parents, Inspiring Elder Brother

&

My Sincere Wife

TABE OF CONTENTS

Chapter 1
Introduction

Chapter 2
Power system stability and its control with FACTS

Chapter 3
Dynamic model of a single machine system with UPFC

Chapter 4
Design of Proportional Integral (PI) controller and Power System Stabilizer (PSS) for UPFC

Chapter 5
Different loading conditions and Eigen Values

Chapter 5
Effect of Model Predictive Controller (MPC) for UPFC connected SMIB

Chapter 7
Conclusion and Future Work

LIST OF FIGURES

LIST OF TABELS

LIST OF SYMBOLS AND ABBREVIATIONS

Abbreviations

FACTS	Flexible AC transmission system
SVC	Static var compensator
TCSC	Thyristor controlled series capacitor
PI	Proportional-integral controller
SMIB	Single machine infinite bus
MPC	Model Predictive Controller
PSS	Power System Stabilizer
TCSC	Thyristor-controlled series capacitor
TCPS	Thyristor-controlled phase shifter
ET, BT	Excitation and boosting transformer
GTO	Gate turn off
VSC	Voltage Source Converters
AVR	Automatic Voltage Regulator
EM	Electromechanical Mode
DTC	Damping Torque Coefficient
Pf	Power Factor
Pu	Per Unit

List of Greek Symbols

δ	Rotor angle
ω	Rotor speed
ω_b	Synchronous speed
δ_E	Excitation phase angle modulation
δ_B	Boosting phase angle modulation
Φ	Phase shift in the voltage phase angle
α	Thyristor firing angle
ζ	Damping ratio
σ	Damping factor

List of English Symbols

d-q	Direct and quadrature axes of generator
r_E, x_E	Resistance and reactance of exciting transformer
r_L, x_L	Resistance and reactance of line including booster transformer
x_d, $x_{d'}$	Synchronous and sub transient armature reactances
x_q	Quadrature axis synchronous reactance
V_E	Sending end line voltage
V_b	Infinite bus voltage
E_q	Voltage behind x_q of the generator
e_B	Voltage across the series (booster) transformer
I_i, I_o	Current input and output of the converter
v_d,v_q	d-q axes generator terminal voltages
i_d, i_q	d-q axes generator armature current

V_t	Generator terminal voltage
V_{to}	Generator terminal reference voltage
V_{dc}	DC-link capacitor voltage
C_{dc}	Capacitance (capacitive reactance) of DC-link capacitor
I_E, I_L	Current in the shunt (exciting) and series (booster) transformer
e_E	Input voltage of VSC-E
m_E, α_E	Modulation index and angle of shunt (excitation) converter
m_B, α_B	Modulation index and angle of series (boosting) converter
P_m, P_e	Input and output power of generator
H, D	Inertia constant and damping coefficient of generator
K_A, T_A	Gain and time constant of exciter and regulator
E_{fd}	Generator field voltage
E_q'	Internal voltage of generator
T_{do}'	Open circuit field time constant
V_{ref}	Reference voltage
V_b	Infinite Bus voltage
U_{PSS}	Control signal of PSS
K_S, T_S	Gain and time constant of FACTS
Z, X, R	Transmission line impedance, reactance and resistance
Y_L	Load impedance
g, b	Load inductance and susceptance
K	Constriction factor

ACKNOWLEDGEMENTS

All praise and glory is due to Allah, the lord, benefactor and cherisher of the entire world who supplied me with the courage, guidance and necessary knowledge to complete this research work. This thesis is a result of research of more than one and a half year and this is by far the most significant scientific accomplishment in my life. It has indeed motivated me to explore more facts and obtain increased knowledge in the field of power system and I would like to continue the research in the future.

I would like to acknowledge those who all helped me to complete this work. The role of the university and the department has been very important and helpful for me during the whole period of research.

I would like to express my heartiest gratitude to my supervisor, Prof. Dr. Md. Shahid Ullah for his great supervision, inspiration and unbounded support for doing this thesis.

I am indebted to Mr. Ashik Ahmed, Asstt. Proff, EEE department, IUT who always kept an eye on the progress of this work and his programming experience was of great benefit for me. I would like to express my deep appreciation and gratitude to him.

Many thanks are due to my departmental teachers specially Prof. Dr. Md. Ashraful Haque and Prof. Dr. Kazi Khairul Islam for their kind involvement and the time they spent to review this thesis.

Special thanks to Prof. Dr. Md. Anwer, Dean, School of Engineering and Computer Science (SECS), Independent University Bangladesh (IUB) for his moral support to carry on the research besides doing my job responsibilities.

Finally my warmest tribute to my parents, beloved wife, all my family members, lots of my friends, seniors, juniors, colleagues and students who every time supported me by their prayers and well wishes for me.

ABSTRACT

This thesis addresses model predictive controller (MPC) as an effective solution for improving the oscillations in a single machine infinite bus (SMIB) power system connected with a FACTS device named unified power flow controller (UPFC). UPFC is mainly used in the transmission systems which can control the power flow by controlling the voltage magnitude, phase angle and impedance. Linearized model of UPFC connected with SMIB system is modeled by five state equations. System oscillations of the plant are attempted to be controlled with power system stabilizer (PSS) and proportional integral (PI) controller. MPC was introduced to damp out the oscillations to improve the performances those of obtained using PSS and PI controller. As a controller, MPC not only provides the optimal control inputs, but also predicts the system model outputs to reach the desired goal. So, model predictive unified power flow controller (MPUPFC), a combination of UPFC and MPC along with proper system model parameters can provide a satisfactory performance in damping out the system oscillations in order to obtain a stable system. Simulation is done in Matlab simulation software. Responses are shown for four different states controlling four different control signals of UPFC.

Chapter 1

Introduction

1.1 Background

Instability means a condition denoting loss of synchronism. So the stability of an interconnected power system is its ability to return to normal or stable operation after having been subjected to some form of disturbance. To obtain and to maintain stability in a power system is very important in the field of power system. Accurate assessment of power system stability has become increasingly important as power systems are stressed to meet the demand of modern market operation [1-2].

Normally the power systems are nonlinear in nature and the operating conditions can vary over a wide range. Recently, small signal stability has received much attention which causes oscillations of a range of 0.1-2 Hz by the small changes in the system. The increasing size of generating units, loading of the transmission lines and high speed excitation systems can become the transmission power limiting factor as these are the main causes affecting the small signal stability. Therefore, system requires a controller to damp out these oscillations. The need for the power flow control in electrical power system is thus evident [2].

In early days, equipments like compensating capacitor, regulating transfer, power system stabilizer (PSS) were used to bring stability in power systems. The continuing rapid development of high-power semiconductor technology now makes it possible to control electric power system by means of power electronic devices. These devices constitute an emerging technology called FACTS (Flexible AC transmission System). FACTS technology has a number of benefits, such as greater power flow control, increased secure loading of existing transmission circuits, damping of power system oscillations, less environmental impact and, potentially, less cost than most alternative techniques of transmission system reinforcement [3-5]. For the analysis of small signal stability accurate representation of system dynamics along with proper FACTS controller is essential.

Among the converter-based FACTS controllers, the unified power flow controller (UPFC) is regarded as one of the most versatile devices in the FACTS device family [6-7] combining the features of the static synchronous compensator (STATCOM) and the static synchronous series compensator (SSSC). It has the ability to control the power flow in the transmission line, improve the transient stability, mitigate system oscillation and provide voltage support. It performs this through the control of the in-phase voltage, quadrate voltage and shunt compensation [8].

The stability of the system can be improved using different controllers, MPC is one of them [9-10]. MPC systems rely on the idea of generating values for process inputs as solutions of an on-line (real-time) optimization problem. MPC system can be modeled for different possibilities of input-output, disturbance prediction, objective, measurement, constraints, and sampling period. Some of the benefits of improved MPC systems are better control performance, less down time, reduced maintenance requirements and improved flexibility.

1.2 Related Work

Several trials have been reported in the literature to model a UPFC for dynamic study. Based on Nabavi-Irani model [11], Wang developed two UPFC models [12, 13] that have been linearized and incorporated into the Heffron-Phillips model [14].

A number of control schemes have been suggested to perform the oscillation-damping task. Huang et al. [15] attempted to design a conventional fixed-parameter lead-lag controller for a UPFC installed in the tie line of a two-area system to damp the multi machine system. Dash et al. [16] suggested the use of a radial basis function for a UPFC to enhance system damping performance. Dash and Mishra suggested neural networks method [16] and robust control methodologies [17, 18] to cope with system uncertainties to enhance the system damping performance using the UPFC.

Also, Limyingcharone and Dash-Mitra used fuzzy logic based damping control strategy for UPFC in a multi-machine power system [19-21]. Chen et al. [22] used a output feedback

controller designed by simulated annealing (SA) for TCSC to improve power system low frequency oscillations. To improve overall system performance, many researches were made on the coordination between PSSs and FACTS damping controllers [23-26]. Some of these methods are based on the complex nonlinear simulation, while the others are based on the linearized power system model.

1.3 Motivation

The main motivation behind doing this work is the attractive features of UPFC and MPC to bring synchronism in an unstable power system. We know, dynamic stability is important from the view point of maintaining system security that is the incidence of a fault should not lead to tripping of generating unit due to loss of synchronism. In earlier days, setups like compensating capacitors or regulating transformers were used in the transmission lines to improve flexibility. Advancement in power electronic devices leads to invent devices like FACTS which has made the task much easier than previous.

In past, many research works have been done by UPFC with other controllers like PSS, PI, neural network and fuzzy logic. Similarly, researches related with MPC combined with different FACTS devices were made. So, the good possibility of finding a better response while using MPC on UPFC in a single machine infinite bus (SMIB) power system is the main motivation behind doing this research.

1.4 Research Objectives

- Develop a non-linear model of SMIB with UPFC through proper mathematical modeling.
- Linearize the model using Taylor series expansion and obtain the state Matrix.
- Performance evaluation of UPFC with Power System Stabilizer (PSS) as well as conventional Proportional Integral (PI) controller on system damping.

- Performance evaluation of the proposed MPUPFC (MPC controller on UPFC) for system damping.

- Comparison of performances between PSS, PI and MPC controllers on system damping.

1.5 Outline of the Thesis

Chapter 1 represents the background of the present work, motivation and objectives and related work with this project.

Chapter 2 elaborates the definition and classification of FACTS devices as well as the effect of UPFC on power system stability control.

Chapter 3 provides the detail modeling of UPFC connected SMIB (both linear and nonlinear).

Chapter 4 describes the design of PI controller and PSS for UPFC as well as the effect of these controllers on system model.

Chapter 5 presents the response characteristics of the system model for different loading conditions as well as the eigen value charts to get an idea about stability.

Chapter 6 describes briefly about MPC, its control strategies and its effect on proposed system model.

Chapter 7 concludes the whole work with a brief summary and some future suggestions.

"Appendices" part has got the list of values used in modeling, constants we got in linearized model and values used in three different loading types.

"Nomenclature" chapter shows all the meanings of symbols (Greek & English) and abbreviations used in the thesis.

Chapter 2

Power system stability and its control with FACTS

2.1 Power System Stability

Modern electric power system is a complex network of synchronous generators, transmission lines and loads. The characteristics of the system vary with changes in load and generation schedules. Electric utilities first grew as isolated systems, and then gradually neighboring utilities began to join forming highly interconnected systems. This enabled the utilities to draw on each other's generation reserves during the time of need. The overall reliability has improved through interconnection but small disturbances in such systems propagate through, leading to system instability and possible black-outs. Systems which have long transmission distances between the load centers and generating stations may exhibit poorly damped or even negatively damped oscillations. If the magnitude of disturbance is large, such as a three phase fault, major line or load switching, the system could even become transiently unstable. A good power system should possess the ability to regain its normal operating condition after a disturbance. Since ability to supply uninterrupted electricity determines the quality of electric power supplied to the load, stability is regarded as one of the important topics of power system research [1, 27-29].

Power system stability can be defined by the ability of synchronous machines to remain in synchronism with each other. The capability of power system to remain in synchronism in the event of possible disturbance such as line faults, generator and line outages and load switching etc., is characterized by its stability. Depending on the order of magnitude and type of disturbances, power system stability can be classified as steady state stability, transient stability and dynamic stability [30-32]. Following unbalances between generation and demand in the system, a power system may experience sustained oscillations. These oscillations may be local to a single generator or they may involve a number of generators widely separated geographically (inter-area oscillations). Local oscillations can occur, for example, when a fast exciter in used on

the generator. Inter area oscillations may appear as the system loading is increased across the weak transmission links. If not controlled, these oscillations may lead to partial or total power interruption [33-35]. Damping the oscillations is not only important in increasing the transmission capability but also for stabilization of power system conditions after critical faults. If the net damping of the system is negative, then the system may lose synchronism. Extra damping has to be provided to the system in order to avoid this. Powerful damping in the system has a twofold advantage of both decreasing the amplitude of first swing and the ratio of each successive swing to the preceding one, thus resulting in overall improvement of stability margin of the system [35-37].

2.2 Methods to damp out the power system oscillations

1. Governor control: Control of input power Pm can stabilize a power system following a disturbance. Though governor control has shown some good results in damping control, it is not accepted by power utilities [28].

2. Excitation control: Among the various methods of damping, excitation control is one of the most common and economical method. Excitation controllers are referred to as power system stabilizers (PSS). PSSs have been thought to improve power system damping by generator voltage regulation depending on system dynamic response [38, 39].

3. Braking Resistors: Braking resistors prevent transient instability by immediately absorbing the real power that would otherwise be used in accelerating the generator. These are very effective to damp the first power system swing [28].

4. Control of the rotor angle (δ): The electrical power output (Pe) can also be altered by varying the rotor angle (δ). Phase shifters can be employed to perform this job.

5. Load shedding: This is the least considered option and is adopted as a last measure.

6. Control of the line reactance: The electrical power output (Pe) can be controlled by controlling the line reactance (X). Reactance control can be achieved by series or shunt compensation. Traditionally these compensators have been fixed, and switched in and out of the system at low

rates. Developments in power electronics have allowed dynamic control of these static shunt and series compensators. Electronically controlled Flexible AC transmission systems (FACTS) devices, discussed in the next section are now being widely used in the power system control.

2.3 Flexible AC Transmission System (FACTS)

From the general point of view, the FACTS principle is mainly dependent on the advanced technologies of power electronic techniques and algorithms into the power system, to make it electronically controllable. FACTS Technology is concerned with the management of active and reactive power to improve the performance of electrical networks. The concept of FACTS technology embraces a wide variety of tasks related to both networks and consumers problems, especially related to power quality issues. In general, the concept of power flow control is concerned with two jobs: load support and voltage compensation. Through the demand operation, the tasks are to raise the amount of the network power factor, to increase the true power from the source, to compensate voltage regulation and to decrease harmonic components resulted from large and fluctuating nonlinear loads especially in industry applications. Voltage Support is mainly important to decrease voltage changes at the terminals of a transmission path.

It also assists to keep a substantially regulated voltage profile at all sections of power transfer, it enhances HVDC (High Voltage Direct Current) feature performance, raises transmission efficiency, sets steady-state bus normal voltage and over voltages, and can avoid serious blackouts [40, 41].

2.3.1 Thyristor Controlled Reactor (TCR) based FACTS devices

The controllable main element present in the basic TCR is two antiparallel thyristor pair (Thy1 & Thy2. Fig 2.1) which conduct on alternate half cycles of the supply frequency. The other key component is the linear (air-core) reactor of inductance L.

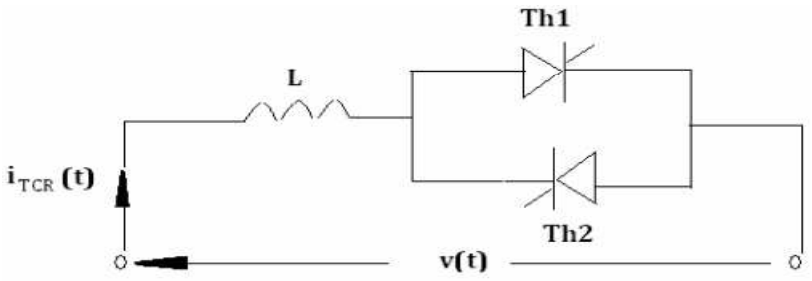

Fig 2.1: The Thyristor Controlled Reactor

A gate pulse is activated to all thyristors of a thyristor valve which brings the valve into conduction. The valve will automatically block approximately at the zero crossing of the AC current, in the absence of the firing signal. Thus, the controlling element is the thyristor valve. The TCR current is essentially reactive, lagging the voltage by nearly 90º.

Among the devices that depend on the TCR are Static Var Compensators (SVC) and Thyristor Controlled Series Capacitor (TCSC).

Static Var Compensator (SVC): The construction of the SVC consists of a TCR in parallel with a capacitors bank. From a technical perspective, the SVC operates as a shunt-connected variable reactance that can produce or draw reactive power to regulate the voltage level at the location of the connection to the system. It is used efficiently to supply fast reactive power and voltage regulation support. The firing angle control of the thyristor provides the SVC with an instantaneous speed of response [42].

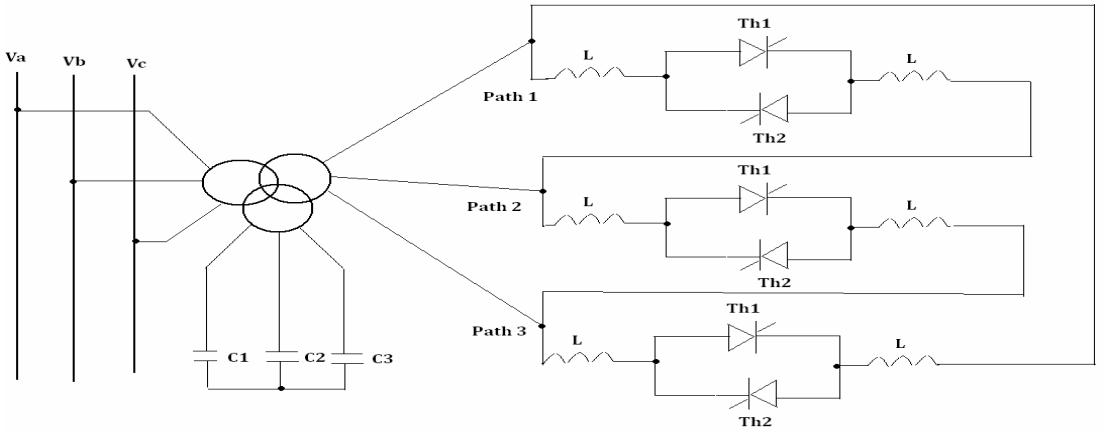

Fig 2.2 : three-phase three winding transformer connected static VAR compensator (SVC)

Thyristor Controlled Series Capacitor (TCSC): A basic TCSC module consists of a TCR in parallel with a capacitor. The TCSC basically comprises a capacitor bank inserted in series with the transmission line, a parallel metal oxide varistor (MOV) to protect the capacitor against over-voltage and a TCR branch, with a thyristor valve in series with a reactor, in parallel with the capacitor. Mechanically bypass breakers are provided in parallel with the capacitor bank and in parallel with the thyristor valve. During normal operation, the bypass switch is open, the bank disconnect switches (1 and 2) are closed and the circuit breaker is open. When it is required to disconnect the TCSC, the bypass circuit breaker is switched on first, and then the bypass switch is switched on. The TCR can be selected to achieve the ability to restrict the voltage at the capacitor at faults and other system contingencies of similar effect [42].

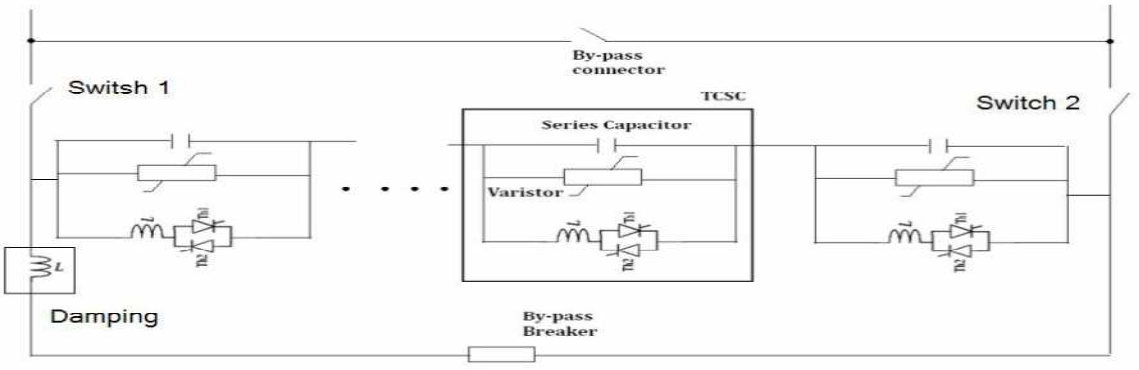

Fig 2.3: Thyristor controlled series capacitor (TCSC)

2.3.2 Synchronous Voltage Source (SVS) based FACTS devices

Controllable solid-state synchronous voltage sources are employed for compensating the dynamic and controlling real-time the power flow in transmission systems. This method, when compared to conventional compensation approaches employing thyristor switched capacitors and thyristor-controlled reactors, saves vastly premium performance characteristics and regular applicability for transmission voltage, reactance, and angle ability. It also gives the powerful tool to exchange active power with the AC grid, in addition to the independently controllable reactive power compensation, thereby giving a powerful new option for the counteraction of dynamic disturbances.

Among the SVS based Facts devises are the STATCOM, the SSSC and the UPFC.

Static Synchronous Compensator (STATCOM): The STATCOM consists of one VSC and its associated shunt-connected transformer. It is the static form of the rotating synchronous condenser but it supplies or draws reactive power with a fast rate because there are no moving parts inside it.

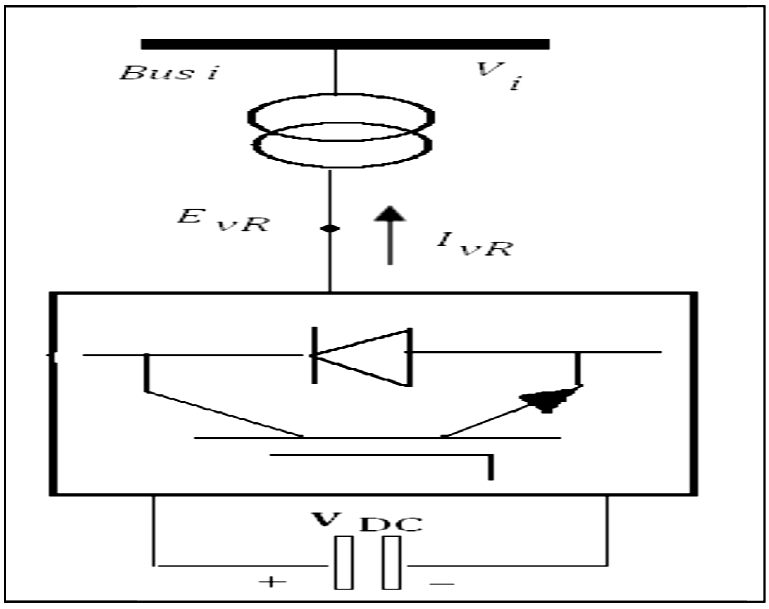

Fig 2.4 : Static compensator (STATCOM) system voltage source converter (VSC) connected to the AC network via a shunt connected transformer

The STATCOM can act as both capacitive and inductive compensators and it is able to control its output current independently over the maximum range of the capacitive or inductive of the network voltage. That is, the STATCOM can produce complete capacitive output current at any grid voltage level. On the other side, the SVC can supply only output current with reducing system voltage as calculated by its maximum equivalent capacitive admittance. So the STATCOM is superior to the SVC in applying voltage support.

Static Series Synchronous Compensator (SSSC): The Static Synchronous Series Compensator (SSSC) is a series connection FACTS controller dependent on VSC. A SSSC own several merits over a TCSC such as (a) elimination of bulky passive components (capacitors and reactors), (b) improved technical characteristics (c) symmetric capability in both inductive and capacitive operating modes (d) the connection availability of an energy source on the DC port to exchange active power with the AC grid.

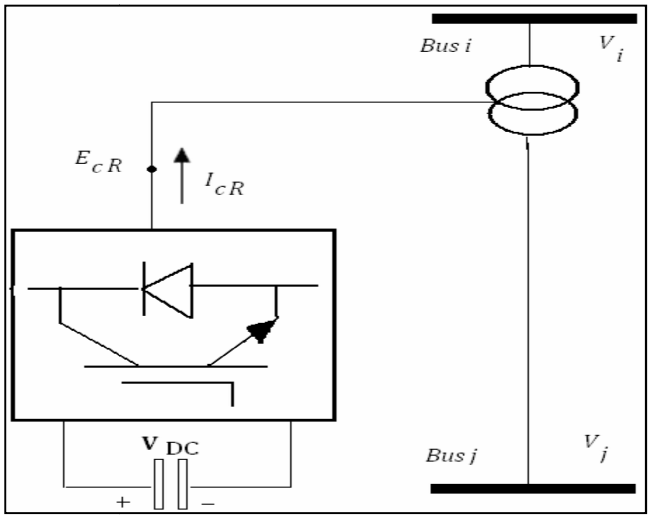

Fig 2.5: Schematic diagram for the SSSC

Unified Power Flow Controller (UPFC): The UPFC may be considered to be constructed of two VSCs sharing a common capacitor on their DC side and a unified control system. That arrangement is practically an achievement of an AC to DC power converter with independently controllable input and output parameters. Additionally, the controller may be adjusted to govern one or more of these criteria in any combination or to control none of them. This technique

permits with the combined application of controlling the phase angle with controlled series reactive compensations and voltage regulation, but also the real-time change from one mode of compensation into another one to handle the actual system contingencies more effectively. For instance, series reactive compensation may be altered by phase-angle control or vice versa.

2.4 Unified Power Flow Controller (UPFC) for power system stability control

The unified power flow controller (UPFC) is the most versatile FACTS device that has emerged for the control and optimization of power flow in electrical power transmission systems. The concept of FACTS was proposed by Gyugyi in 1991 [3]. The UPFC offers major potential advantages for the static and dynamic operation of transmission lines since it combines the features of both the Static Synchronous Compensators (STATCOM) and the Static Synchronous Series Compensator (SSSC). The UPFC is able to control, simultaneously or selectively, all the parameters affecting power flow in the transmission line - voltage, impedance, and phase angle; and this unique capability is signified by the adjective "unified" in its name. Alternatively, it can independently control both the real and reactive power flow in the line.

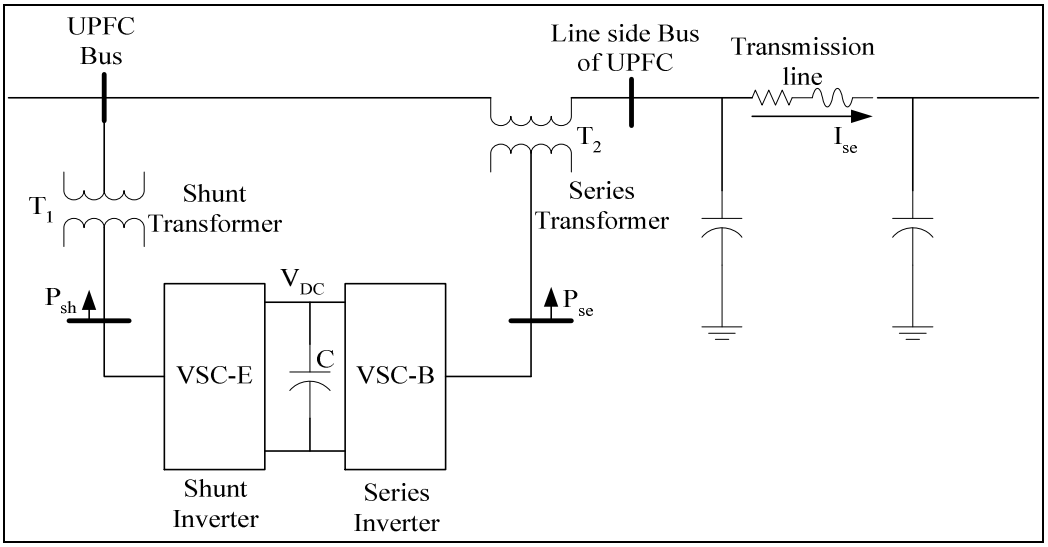

Fig. 2.6: Structure of UPFC

The UPFC consists of two voltage source converters (VSCs), as shown in figure 2.6. The back-to-back converters, labeled 'VSC-E' and 'VSC-B' in the figure, are operated from a common dc link provided by a dc storage capacitor. This arrangement functions as an ideal ac-to-ac power converter in which real power can freely flow in either direction between the ac terminals of the two converters, and each converters can independently generate (or absorb) reactive power at its own ac terminal. VSC-B provides the main function of the UPFC by injecting a voltage (of variable magnitude) in series with the line via an insertion transformer. This injected voltage acts essentially as a synchronous ac voltage source. The current flowing through this voltage source results in reactive and real power exchange between it and the ac system. The reactive power exchange at the ac terminal is generated internally by the converter. The real power exchange at the ac terminal is converted into dc power, which appears at the dc link as a positive or negative real power demand.

The basic function of VSC-E is to supply or absorb the real power demanded by VSC-B at the common dc link to support the real power exchange resulting from the series voltage injection. The dc link power demand of VSC-B is converted back to ac by VSC-E and coupled to the transmission line bus via a shunt-connected transformer. In addition to the real power need of VSC-B, VSC-E can also generate or absorb controllable reactive power, if it is desired, and thereby provide independent shunt reactive compensation for the line.

UPFC can be used for power flow control, loop flow control, load sharing among parallel corridors, providing voltage support, enhancement of transient stability, mitigation of system oscillations, etc. The stability and damping control aspect of an UPFC has been investigated by a number of researchers. The additional damping control circuits can be installed along with normal power flow controllers. Most of the control studies are based on linearized models of the nonlinear power system dynamics [43-44]. These include EL (exact linearization), LQR (linear quadratic regulator) theory, DFL (direct feedback linearization). Stabilizers based on conventional control theory with fixed parameters can be very well tuned to a particular operating condition and provide excellent damping under that condition, but the highly non-linear, wide range operation and stochastic properties of the actual power system present the following problems to the fixed parameter controllers -

- How to choose a transfer function for the controller that gives satisfactory supplementary stabilizing signal covering all frequency ranges of interest

- How to effectively tune the controller parameters

- How to automatically track the variation of the system operating conditions

- How to consider the interaction between the various machines of an interconnected system.

Considering the above points, it is desirable to develop a controller which has the ability to adjust its own parameters, finding the system structure or model on-line according to the environment in which it works to yield satisfactory control performance.

2.5 Control Strategies of UPFC

UPFC basic control design involves control of real and reactive power flow, sending bus voltage magnitude and DC voltage control. The most frequently used control scheme is based on the vector-control approach proposed by Schauder and Metha in 1991 [42]. This scheme allows decoupled control of the real and reactive powers which makes it suitable for UPFC application. This control scheme can be applied both for series and shunt converter control [46]. The shunt converter can be controlled using two PI controllers for the sending bus voltage magnitude and the dc link voltage controls [47]. In [48], a decoupled control strategy based on [45] is proposed and the UPFC behavior is simulated for a short time frame. The study mainly concerns the internal control and dynamics of UPFC and the interface of UPFC with the power system, is not considered.

The supplementary controls of UPFC are applied to the shunt inverter through the modulation of voltage magnitude reference signal or to the series inverter through modulation of power reference signal. In [49], the slip of the desired machine (i.e. $\Delta\omega$) is used as the input signal to the damping controller. In general it is difficult to obtain this signal as most FACTS devices are usually installed on a transmission line far away from any generator. Since, this kind of control is not feasible, and controllers depending on local measurements such as tie-line power flow or the

UPFC terminal voltage phase angle difference are proposed [45]. Padiyar and Kulkarni [47] have proposed a UPFC control strategy based on local measurements, in which the real power flow through the line is controlled by reactive voltage injection and reactive power flow is controlled by regulating the magnitude of the voltages at the two UPFC ports. Padiyar and Rao [41] presented a control scheme for the series compensation voltage of the UPFC to enhance system damping and improve transient stability of the system. The feedback control to determine the shunt compensation is not integrated into the analytical model and the dynamics of the DC link voltage was ignored. Tambey and Kothari [7] presented a gradient-type Newton algorithm for UPFC controller design.

All the controllers referenced above are of lead-lag type. They are designed for a specific operating condition using linearized model. However, changes in operating conditions might have negative effect on the controller performance. More advanced control schemes such as self-tuning control, sliding-mode control, and fuzzy logic control offer better dynamic performance over the conventional controllers.

Self tuning adaptive control schemes are very suitable for systems with non-linearities. Their identify-then-control approach can address the robustness performance through on-line adjustment of controller parameters to ensure acceptable performance for coarsely known plants. In [47], D. A. Pierre have given a perspective on adaptive control of power system. O. P. Malik et al have published a series of papers on adaptive power system stabilizers (PSS) based on pole-shifting technique [48-49]. The use of microprocessor based adaptive load frequency control is presented in [50]. It is worth mentioning here that artificial neural networks (ANNs) have also good potential for system identification and adaptive control since they are able to cope with severe non-linearity.

Reason behind choosing MPC in this thesis to control UPFC is the attractive features of MPC which are described in brief in chapter 06. Capability to deal with multiple inputs and providing multiple outputs has made this controller different from others.

Chapter 3

Dynamic model of a single machine system with UPFC

3.1 Single machine infinite bus (SMIB) system modeling

An infinite bus is a source of invariable frequency and voltage (both in magnitude and angle). A major bus of a power system of very large capacity compared to the rating of the machine under consideration is approximately an infinite bus. The inertia of the machines in large systems will make the bus voltage of many high-voltage buses essentially constant. A remote power station connected to a load centre through a long transmission line can be approximated by single machine infinite bus (SMIB) system. Normally a power station consists more than one generator but those can be represented as an equivalent machine. A schematic representation of this system is shown below.

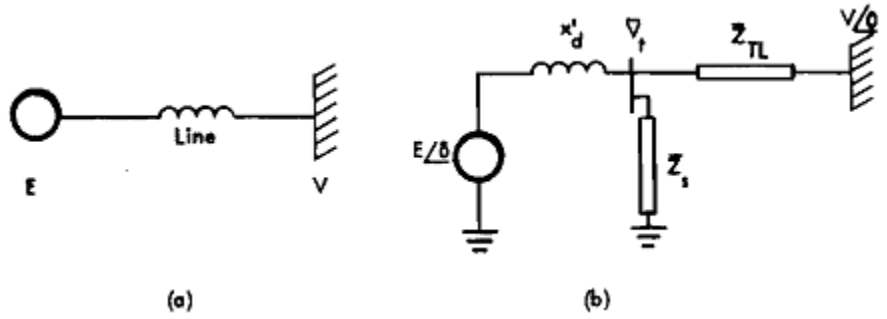

Fig 3.1: One machine connected to an infinite bus through the transmission line (a) one line diagram, (b) equivalent circuit

3.1.1 Non linear model of Single Machine Infinite Bus (SMIB) system

A power system consisting of one machine (generator) connected to an infinite bus has been considered here for the system model.

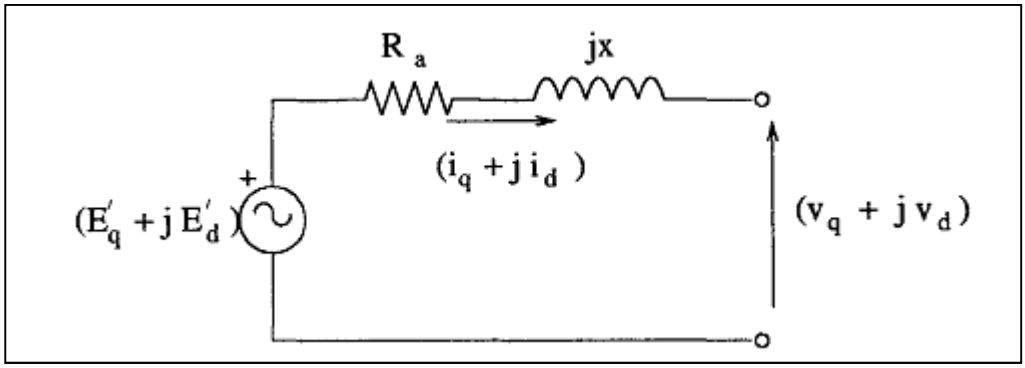

Fig 3.2: stator equivalent circuit

From the figure 3.2, it has been seen that a voltage source ($E_q^{'}$+j$E_d^{'}$) is present behind the equivalent impedance (R_a+jx_a). The stator equation of generator is like this:

$$V_q = E_q^{'} - i_q R_a + x_d{}' i_d \tag{3.1.1}$$

$$V_d = E_d^{'} - i_d R_a - x_q{}' i_q \tag{3.1.2}$$

Where v_d , v_q are the d-q axes generator terminal voltages. And i_d, i_q are the d-q axes armature currents respectively.

If V_t and E_b is the generator terminal voltage and bus voltage respectively, then the network equation will be like this:

$$V_t = Z_e i + E_b$$

$$=>V_d + jV_q = \left(r_e i_d - x_e i_q\right) + j\left(x_e i_d + r_e i_q\right) + E_b Cos\delta + jE_b Sin\delta \quad (3.1.3)$$

Here, δ is the rotor angle.

Equating real and imaginary part of eq^n (3), we get

$$V_d = r_e i_d - x_e i_q + E_b Cos\delta \quad (3.1.4)$$

$$V_q = x_e i_d + r_e i_q + E_b Sin\delta \quad (3.1.5)$$

Comparing eq^n (3.3.1-3.1.2) & (3.1.4-3.1.5), we get

$$i_d(x_d{}' - x_e) + i_q(-r_e - R_a) = E_b Sin\delta - E_q^{'} \quad (3.1.6)$$

$$i_d\left(-x_q^{'} + x_e\right) + i_q(-r_e - R_a) = E_b Cos\delta - E_d^{'} \quad (3.1.7)$$

From equation (3.1.6) and (3.1.7) we can write

$$\begin{bmatrix} i_d \\ i_q \end{bmatrix} \begin{bmatrix} (x_d{}' - x_e) & (-r_e - R_a) \\ (-r_e - R_a) & \left(-x_q^{'} + x_e\right) \end{bmatrix} = \begin{bmatrix} E_b Sin\delta - E_q^{'} \\ E_b Cos\delta - E_d^{'} \end{bmatrix} \quad (3.1.8)$$

If we apply Cramer's rule in equation (3.1.8), then we can find the non-state variables id and iq.

$$i_q = \frac{(r_e + R_a)\left(-E_b Cos\delta + E_q^{'}\right) + \left(x_d^{'} + x_e\right)\left(E_b Sin\delta + E_d^{'}\right)}{det} \quad (3.1.9)$$

$$i_d = \frac{(r_e + R_a)\left(E_b Sin\delta + E_d^{'}\right) + \left(-x_q^{'} - x_e\right)\left(-E_b Cos\delta + E_q^{'}\right)}{det} \quad (3.1.10)$$

Here, the determinant, $det = (r_e + R_a)^2 + \left(x_q^{'} + x_e\right)\left(x_d^{'} + x_e\right)$

The synchronous generator is modeled through q-axis component of transient voltage and electromechanical swing equation representing motion of the rotor. The internal voltage equation of the generator is written as,

$$\dot{E}_q^{'} = \frac{1}{T_{do}^{'}}[E_{fd} - E_{qo}^{'} - (x_d - x_d^{'})i_d] \tag{3.1.11}$$

$$E_d\dot{\square} = \left[-E_d\square - (x_q - x_q{}')i_q\right]\frac{1}{T_{q0}}$$

(3.1.12)

Where, xd, xd′ and T'_{d0} are the d-axis synchronous reactance, transient reactance and open circuit field constants, respectively.

The electromechanical swing equation is broken into two first order differential equations and is written as,

$$\dot{\omega} = \frac{1}{2H}[P_m - P_e - D(\omega - 1)] \tag{3.1.13}$$

$$\dot{\delta} = \omega_{base}(\omega - 1) \tag{3.1.14}$$

Where P_m is the mechanical power input. H is the inertia constant in seconds and ω_{base} is the synchronous speed.

The electrical power output is, $P_e = v_d\, i_d + v_q\, i_q$

Considering negligible armature resistance we can write the d and q components of the generator terminal voltage as :

$$\begin{aligned} v_d &= x_q i_q = x_q\left(i_{iq} + i_{lq}\right) \\ v_q &= E_q{}' - x_d{}' i_d = e_q{}' - x_d\left(i_{id} + i_{ld}\right) \end{aligned} \tag{3.1.15}$$

The generator terminal voltage (v_t) in terms of the state variables:

$$v_t = \sqrt{\left(v_d^2 + v_q^2\right)}$$
$$= \sqrt{\left(x_q^2\left(i_{iq} + i_{lq}\right)^2 + e_q{}'^2 - 2x_d{}'e_q{}'\left(i_{id} + i_{ld}\right) + x_d^2\left(i_{id} + i_{ld}\right)^2\right)} \quad (3.1.16)$$

3.1.2 Excitation system and Power System Stabilizer (PSS)

The main objective of the excitation system is to control the field voltage of the synchronous machine. The field voltage is controlled so as to regulate the terminal voltage of the machine. The IEEE type STI is used for the voltage regulator excitation. The block diagram of the excitation system is shown in Fig. 3.3.

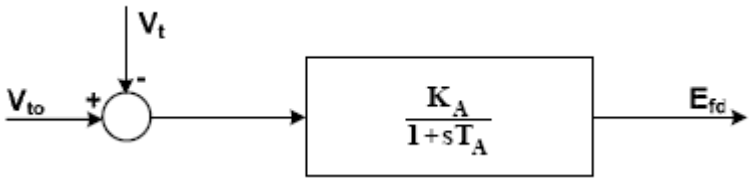

Fig 3.3: Block diagram of excitation system

The dynamic model of the excitation system is,

$$\Delta\dot{E}_{fd} = K_A((V_{ref} - v + U_{pss}) - E_{fd})\frac{1}{T_A} \quad (3.1.17)$$

Where, K_A and T_A are the gain and time constant of exciter, respectively. V_{ref} represents the reference terminal voltage of generator. E_{fd} is the field voltage.

A cost efficient and satisfactory solution to the problem of oscillatory instability is to provide damping for generator rotor oscillations. This is conveniently done by providing Power System Stabilizers (PSS) which are supplementary controllers in the excitation systems. The output signal from PSS which has input signal derived from rotor velocity, frequency, electrical power or a combination of these variables. The objective of designing PSS is to provide additional damping torque without affecting the synchronizing torque at critical oscillation frequencies.

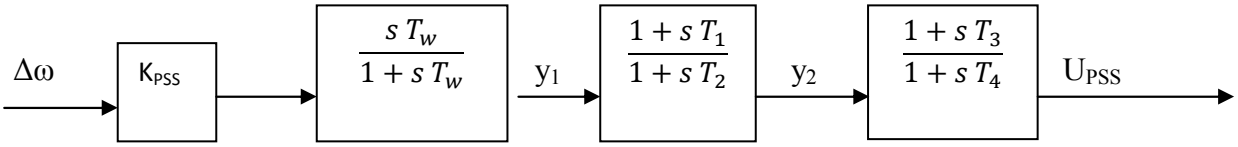

Fig 3.4: Block representation of power system stabilizer (PSS)

From the figure 3.4 we get 3 more state equations like this

$$\dot{y_1} = [K_{PSS}\,\dot{w}\,T_w - y_1]\frac{1}{T_w} \tag{3.1.18}$$

$$\dot{y_2} = [\dot{y_1}\,T_1 + y_1 - y_2]\frac{1}{T_2} \tag{3.1.19}$$

$$\dot{\boldsymbol{U_{PSS}}} = [\boldsymbol{\dot{y}_2\,T_3 + y_2 - U_{PSS}}]\frac{\boldsymbol{1}}{\boldsymbol{T_4}} \tag{3.1.20}$$

Where, U_{PSS} is the output signal from PSS.

3.1.3 SMIB system linearized model

If we now linearize the state equations of DAE model (eq^n 3.1.11-3.1.14, 3.1.17) then we will get the equations like this

$$\Delta\delta = \dot{w}_0 \Delta w$$

$$\Delta \dot{w} = \Delta E_q' \, K_2 + \Delta \, \delta \, K_1 + \Delta E_d' K_9$$

$$\Delta \dot{E_q}' = \Delta E_q' K_6 + \Delta \, \delta \, K_5 + \Delta E_d' K_{10} + \Delta E_{fd}$$

$$\Delta \dot{E_d}' = \Delta E_q' K_8 + \Delta \, \delta \, K_7 + \Delta E_d' K_{11}$$

$$\Delta \dot{E_{fd}} = \Delta E_q' K_4 + \Delta \, \delta \, K_3 + \Delta E_d' K_{12} - \frac{\Delta Efd}{T_A}$$

Here (K_1-K_{11}) are the constants.

From the equations written above, we can form the state matrix like $\dot{X} = A\,X$.

3.2 Single-machine infinite-bus system with UPFC

3.2.1 Description of UPFC installed SMIB system

Now, we are going to model a SMIB (Single Machine Infinite Bus) system which is having a UPFC installed between the secondary side of the sending end transformer and the Infinite bus having a voltage (Vb). The primary side of the sending end transformer is connected to the generator (G). Xt is the transformer reactance in p.u. The terminal voltage V_t is controllable by the UPFC parameters.

The UPFC itself consists of an Excitation transformer (ET) and a Booster Transformer (BT) which are in parallel and series with the system transmission line respectively. Two Voltage source converters (VSCs) (one of them working as a rectifier and the other one as an inverter) are coupled by a dc capacitor. The booster transformer carries the same current I_B as that of the

transmission line and is transformed into output current to represent the current through the inverter/output converter whereas the excitation transformer carries I_E and transforms it to input current which flows into the rectifier/input converter. Operation of the converters is greatly influenced by their amplitude modulation indices and phase angles which can be controlled by well-established methods. The simplified system model is as shown in Fig. 3.4

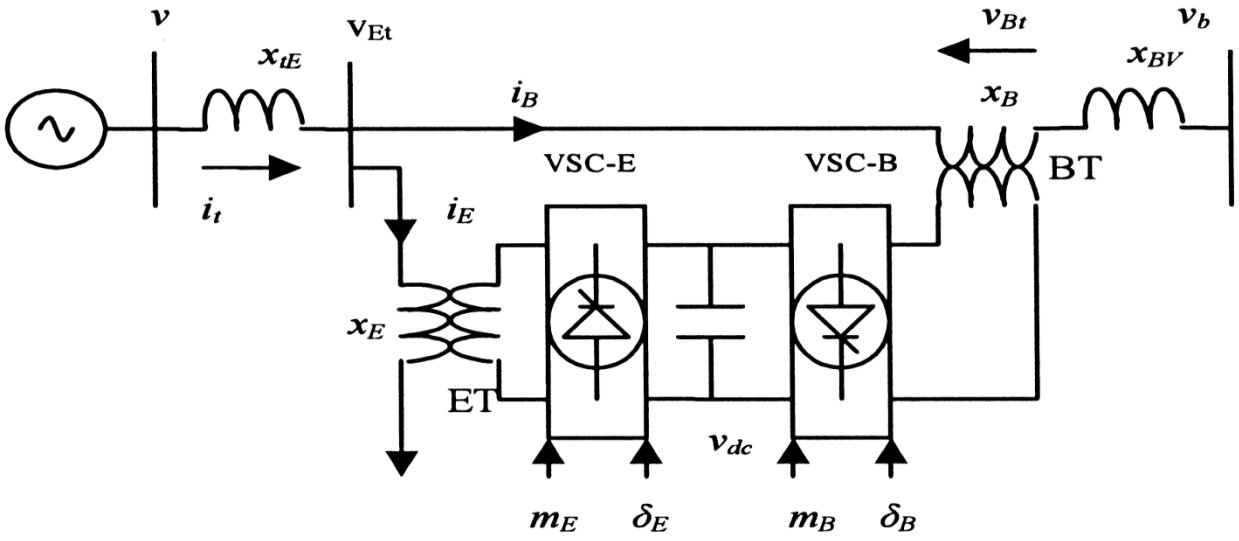

Fig 3.4: SMIB power system equipped with UPFC

3.2.2 Nonlinear model

By applying Park's transformation and neglecting the resistance and transients of the excitation transformer and boosting transformer, the UPFC can be modeled as [51-54],

$$\overline{V_E} = \frac{m_E V_{DC}}{2} e^{j\delta E}$$

$$=> V_{Ed} + j\, V_{Eq} = \frac{m_E V_{DC}}{2} (Cos\delta_E + j\, Sin\delta_E)$$

$$\begin{bmatrix} v_{Etd} \\ v_{Etq} \end{bmatrix} = \begin{bmatrix} o & -x_E \\ x_E & 0 \end{bmatrix} \begin{bmatrix} i_{Ed} \\ i_{Eq} \end{bmatrix} + \begin{bmatrix} \frac{m_E \cos\delta_E v_{dc}}{2} \\ \frac{m_E \sin\delta_E v_{dc}}{2} \end{bmatrix} \quad (3.2.1)$$

Similarly, $\overline{V_E} = \frac{m_B V_{DC}}{2} e^{j\delta B}$

$$\Rightarrow \begin{bmatrix} v_{Btd} \\ v_{Btq} \end{bmatrix} = \begin{bmatrix} o & -x_B \\ x_B & 0 \end{bmatrix} \begin{bmatrix} i_{Bd} \\ i_{Bq} \end{bmatrix} + \begin{bmatrix} \frac{m_B \cos\delta_B v_{dc}}{2} \\ \frac{m_B \sin\delta_B v_{dc}}{2} \end{bmatrix} \quad (3.2.2)$$

$$\dot{v}_{dc} = \frac{3m_E}{4C_{dc}}(\cos\delta_E i_{Ed} + \sin\delta_E i_{Eq}) + \frac{3m_B}{4C_{dc}}(\cos\delta_B i_{Bd} + \sin\delta_B i_{Bq}) \quad (3.2.3)$$

Where V_E and V_B are the excitation and boosting voltages respectively. i_{Ed}, $i_{Eq,}$ $i_{Bd,}$ i_{Bq} are the d-q components of excitation and boosting current, respectively. C_{dc} and V_{DC} are the DC link capacitance and voltage, respectively.

And the four input control signals to the UPFC are m_E, m_B, δ_E, and δ_B, where
m_E and m_B are the excitation and boosting amplitude modulation ratio,
δ_E and δ_B are the excitation and boosting phase angle.

Now, from the figure (3.4) we can write, $\bar{v} = j\, x_{tE} \bar{\imath_t} + \overline{v_{Et}}$

$$\Rightarrow V_d + jV_q = j\, X_{tE}\,(i_d + j\, i_q) + (V_{Etd} + j\, V_{Etq})$$

$$\Rightarrow V_d + jV_q = j\, X_{tE}\,(i_{Ed} + i_{Eq} + j\, i_{Bd} + j\, i_{Bq}) + (V_{Etd} + j\, V_{Etq}) \quad (3.2.4)$$

Again, $\overline{V_t} = V_d + jV_q$

$$\Rightarrow \overline{V_t} = x_q i_q + j\,[E_q' - x_d' i_d]$$

$$\Rightarrow \overline{V_t} = X_q\,(i_{Eq} + i_{Bq}) + j\,[E_q' - x_d'\,(i_{Ed} + i_{Bd})] \quad (3.2.5)$$

Equating real and imaginary part of equation (3.2.3), (3.2.4) and using the value of (3.2.1) we get

$$X_q\, i_{Eq} + X_q\, i_{Bq} = -\, X_{tE}\, i_q - X_E\, i_{Eq} + \frac{m_E \cos\delta_E V_{DC}}{2} \quad (3.2.6)$$

$$E_q' - x_d'\, i_{Ed} - x_d'\, i_{Bd} = -\, X_{tE}\, i_d + X_E\, i_{Ed} + \frac{m_E \sin\delta_E V_{DC}}{2} \quad (3.2.7)$$

Again, from the figure (3.4), we can write $\overline{v_{Et}} = \overline{v_{Et}} + j\, x_{BV} \bar{\imath_B} + \overline{v_B}$

⇨ $(V_{Etd} + j\, V_{Etq}) = V_{Btd} + j\, V_{Btq} + j\, X_{BV}\,(i_{Bd} + j\, i_{Bq}) + V_b \sin\delta + j\, V_b \cos\delta$

⇨ $(-X_E\, i_{Eq} + \frac{m_E \cos\delta_E\, v_{DC}}{2}) + j\,(X_E\, i_{Ed} + \frac{m_E \sin\delta_E\, v_{DC}}{2}) = (-X_B\, i_{Bq} + \frac{m_B \cos\delta_B\, v_{DC}}{2} - X_{BV}\, i_{Bq} +$

$V_b \sin\delta) + j\,(X_B\, i_{Bd} + \frac{m_B \sin\delta_B\, v_{DC}}{2} + X_{BV}\, i_{Bd} + V_b \cos\delta)$ (3.2.8)

Equating real and imaginary part of (3.2.7), we get

$$-X_E\, i_{Eq} + \frac{m_E \cos\delta_E\, v_{DC}}{2} = -X_B\, i_{Bq} + \frac{m_B \cos\delta_B\, v_{DC}}{2} - X_{BV}\, i_{Bq} + V_b \sin\delta \quad (3.2.9)$$

$$X_E\, i_{Ed} + \frac{m_E \sin\delta_E\, v_{DC}}{2} = X_B\, i_{Bd} + \frac{m_B \sin\delta_B\, v_{DC}}{2} + X_{BV}\, i_{Bd} + V_b \cos\delta \quad (3.2.10)$$

Solving the equations (3.2.5, 3.2.6, 3.2.8 & 3.2.9), we get four equations for current:

$$i_{Ed} = \frac{x_{BB}}{x_{d\Sigma}} E_q' - \frac{m_E Sin\delta_E v_{dc} x_{Bd}}{2x_{d\Sigma}} + \frac{x_{dE}}{x_{d\Sigma}}(v_b Cos\delta + \frac{m_B Sin\delta_B v_{dc}}{2}) \quad (3.2.11)$$

$$i_{Eq} = \frac{m_E Cos\delta_E v_{dc} x_{Bq}}{2x_{q\Sigma}} - \frac{x_{qE}}{x_{q\Sigma}}(v_b Sin\delta + \frac{m_B Sin\delta_B v_{dc}}{2}) \quad (3.2.12)$$

$$i_{Bd} = \frac{x_E}{x_{d\Sigma}} E_q' + \frac{m_E Sin\delta_E v_{dc} x_{dE}}{2x_{d\Sigma}} - \frac{x_{dt}}{x_{d\Sigma}}(v_b Cos\delta + \frac{m_B Sin\delta_B v_{dc}}{2}) \quad (3.2.13)$$

$$i_{Bq} = -\frac{m_E Cos\delta_E v_{dc} x_{qE}}{2x_{q\Sigma}} + \frac{x_{qt}}{x_{q\Sigma}}(v_b Sin\delta + \frac{m_B Cos\delta_B v_{dc}}{2}) \quad (3.2.14)$$

Where, $x_{qt} = x_q + x_{tE} + x_E$, $x_{qE} = x_q + x_{tE}$,

$x_{dt} = x'_d + x_{tE} + x_E$, $x_{dE} = x'_d + x_{tE}$, $x_{BB} = x_B + x_{BV}$

$x_{q\sum} = x_{qt}\ x_{BB} + x_e\ x_{qE} = (x_q + x_{tE} + x_E)(x_B + x_{BV}) + x_e(x_q + x_{tE})$,

$x_{Bq} = x_{BB} + x_{qE} = x_B + x_{BV} + x_q + x_{tE}$

$x_{d\sum} = x_{dt}\ x_{BB} + x_E\ x_{dE} = (x'_d + x_{tE} + x_E)(x_B + x_{BV}) + x_E(x'_d + x_{tE})$,

$x_{Bd} = x_{BB} + x_{dE} = x_B + x_{BV} + x'_d + x_{tE}$

Here, X_E and X_B are the ET and BT reactance, respectively.
And the non linear model of SMIB system (fig. 3.4) can be described by the following state equations:

$$\dot{\omega} = \frac{1}{2H}[P_m - P_e - D(\omega - 1)] \tag{3.1.15}$$

$$\dot{\delta} = \omega_{base}(\omega - 1) \tag{3.1.16}$$

$$\dot{E}'_q = \frac{1}{T'_{do}}[E_{fd} - E'_{qo} - (x_d - x'_d)i_d] \tag{3.1.11}$$

$$\Delta\dot{E}_{fd} = K_A((V_{ref} - v + U_{pss}) - E_{fd})\frac{1}{T_A} \tag{3.1.17}$$

3.2.3 Linearized model

The power system model described in the previous section is nonlinear. For designing the controller, it is usually more convenient to use the linearized model of SMIB.

From equation (3.2.11), we know that the d-component of current passing through ET is,

$$i_{Ed} = \frac{x_{BB}}{x_{d\sum}}E_q' - \frac{m_E Sin\delta_E v_{dc} x_{Bd}}{2x_{d\sum}} + \frac{x_{dE}}{x_{d\sum}}(v_b Cos\delta + \frac{m_B Sin\delta_B v_{dc}}{2})$$

⇨ $\Delta i_{Ed} = -\frac{X_{dE}V_{b0}Sin\,\delta_0}{X_{d\Sigma}}\,\Delta\delta + \frac{X_{BB}}{X_{d\Sigma}}\,\Delta E'_q + (\frac{X_{dE}m_B Sin\,\delta_B}{2X_{d\Sigma}} - \frac{X_{Bd}m_E Sin\,\delta_E}{2X_{d\Sigma}})\,\Delta V_{dc} - \frac{X_{Bd}V_{dc}Sin\,\delta_E}{2X_{d\Sigma}}$

$\Delta m_E - \frac{mE\,X_{Bd}V_{dc}Cos\,\delta_E}{2X_{d\Sigma}}\,\Delta\delta_E + \frac{X_{dE}V_{dc}Sin\,\delta_B}{2X_{d\Sigma}}\,\Delta m_B + \frac{mB\,X_{dE}V_{dc}Cos\,\delta_B}{2X_{d\Sigma}}\,\Delta\delta_B$

⇨ $\Delta i_{Ed} = B_1\,\Delta\delta + B_2\,\Delta E'_q + B_3\,\Delta V_{dc} + B_4\,\Delta m_E + B_5\,\Delta\delta_E + B_6\,\Delta m_B + B_7\,\Delta\delta_B$

⇨ $\Delta i_{Ed} = [B_1\ \ B_2\ \ B_3\ \ B_4\ \ B_5\ \ B_6\ \ B_7]\ X\ [\Delta\delta;\ \Delta E'q;\ \Delta Vdc;\ \Delta mE;\ \Delta\delta E;\ \Delta mB;\ \Delta\delta B]$

⇨ $\Delta i_{Ed} = [B_1\ \ B_2\ \ B_3\ \ B_4\ \ B_5\ \ B_6\ \ B_7]\ X\ \Delta X_u$ (3.2.15)

Here, ΔX_u is a (7X1) matrix.

Similarly, from equation (3.2.13),

$\Delta i_{Bd} = B_8\,\Delta\delta + B_9\,\Delta E'_q + B_{10}\,\Delta V_{dc} + B_{11}\,\Delta m_E + B_{12}\,\Delta\delta_E + B_{13}\,\Delta m_B + B_{14}\,\Delta\delta_B$

⇨ $\Delta i_{Bd} = [B_8\ \ B_9\ \ B_{10}\ \ B_{11}\ \ B_{12}\ \ B_{13}\ \ B_{14}]\ X\ \Delta X_u$ (3.2.16)

Now, $i_d = i_{Ed} + i_{Bd}$

⇨ $\Delta i_d = B_{15}\,\Delta\delta + B_{16}\,\Delta E'_q + B_{17}\,\Delta V_{dc} + B_{18}\,\Delta m_E + B_{19}\,\Delta\delta_E + B_{20}\,\Delta m_B + B_{21}\,\Delta\delta_B$

⇨ $\Delta i_d = [B_{15}\ \ B_{16}\ \ B_{17}\ \ B_{18}\ \ B_{19}\ \ B_{20}\ \ B_{21}]\ X\ \Delta X_u$ (3.2.17)

From (3.2.12)

⇨ $\Delta i_{Eq} = [B_{22}\ \ B_{23}\ \ B_{24}\ \ B_{25}\ \ B_{26}\ \ B_{27}\ \ B_{28}]\ X\ \Delta X_u$ (3.2.18)

From (3.2.12)

⇨ $\Delta i_{Bq} = [B_{29}\ \ B_{30}\ \ B_{31}\ \ B_{32}\ \ B_{33}\ \ B_{34}\ \ B_{35}]\ X\ \Delta X_u$ (3.2.19)

Now, $i_q = i_{Eq} + i_{Bq}$

⇨ $\Delta i_d = [B_{36}\ \ B_{37}\ \ B_{38}\ \ B_{39}\ \ B_{40}\ \ B_{41}\ \ B_{42}]\ X\ \Delta X_u$ (3.2.20)

We know, $v_d = x_q i_q$

⇨ $\Delta V_d = [B_{43} \quad B_{44} \quad B_{45} \quad B_{46} \quad B_{47} \quad B_{48} \quad B_{49}] \; X \; \Delta X_u$ (3.2.21)

And $v_q = E_q' - x_d' i_d$

⇨ $\Delta V_q = [B_{50} \quad B_{51} \quad B_{52} \quad B_{53} \quad B_{54} \quad B_{55} \quad B_{56}] \; X \; \Delta X_u$ (3.2.22)

The constants B_1-B_{56} are the functions of X_{tE}, X_E, X_B, X_{BV}, C_{dc}, E'_{q0}, V_{dc0}, X'_d, X_q, i_{d0}, i_{q0}, m_{E0}, m_{B0}, δ_{E0}, δ_{B0}.

Now, by linearizing P_e, $\dot{E}_q'$, V_t and V_{dc}, we will get the K constants.

$$P_e = v_d i_d + v_q i_q$$

⇨ $\Delta P_e = [K_1 \quad K_2 \quad K_{pd} \quad K_{pe} \quad K_{pde} \quad K_{pb} \quad K_{pbd}] \; X \; \Delta X_u$ (3.2.23)

From equation (3.1.11), we get a linearized form like this

$\Delta \dot{E}_q' = [K_4 \quad K_3 \quad K_{qd} \quad K_{qe} \quad K_{qde} \quad K_{qb} \quad K_{qbd}] \; X \; \Delta X_u$ (3.2.24)

From equation (3.1.16), $v_t = \sqrt{\left(v_d^2 + v_q^2\right)}$

⇨ $2 V_{t0} \Delta V_t = 2V_{d0} \Delta V_d + 2V_{q0} \Delta Vq$

⇨ $\Delta V_t = \left(\frac{Vd0}{Vt0} + \frac{Vq0}{Vt0} \right)$

⇨ $\Delta V_t = [K_5 \quad K_6 \quad K_{vd} \quad K_{ve} \quad K_{vde} \quad K_{vb} \quad K_{vbd}] \; X \; \Delta X_u$ (3.2.25)

And finally, linearizing equation (3.2.3) we get

$\Delta V_{dc} = [K_7 \quad K_8 \quad -K_9 \quad K_{ce} \quad K_{cde} \quad K_{cb} \quad K_{cbd}] \; X \; \Delta X_u$ (3.2.26)

Here, the K constants are the functions of B_1-B_{56}.

In state-space representation, the power system can be modeled as

$$\dot{X} = A\Delta X + B\Delta U$$

where the state vector ΔX and control vector ΔU are

$\Delta X = [\Delta\delta \quad \Delta\omega \quad \Delta E'_q \quad \Delta E_{fd} \quad \Delta V_{dc}]^T$
$\Delta U = [\Delta U_{pss} \quad \Delta m_E \quad \Delta\delta_E \quad \Delta m_B \quad \Delta\delta_B]^T$

The constants

$$A = \begin{bmatrix} 0 & \omega_b & 0 & 0 & 0 \\ -\frac{K_1}{M} & -\frac{D}{M} & -\frac{K_2}{M} & 0 & -\frac{K_{pd}}{M} \\ -\frac{K_4}{T'_{d0}} & 0 & -\frac{K_3}{T'_{d0}} & \frac{1}{T'_{d0}} & -\frac{K_{qd}}{T'_{d0}} \\ -\frac{K_A K_5}{T_A} & 0 & -\frac{K_A K_6}{T_A} & -\frac{1}{T_A} & -\frac{K_A K_{vd}}{T_A} \\ K_7 & 0 & K_8 & 0 & -K_9 \end{bmatrix}$$

and

$$B = \begin{bmatrix} 0 & 0 & 0 & 0 & 0 \\ 0 & -\frac{K_{pe}}{M} & -\frac{K_{pde}}{M} & -\frac{K_{pb}}{M} & -\frac{K_{pdb}}{M} \\ 0 & -\frac{K_{qe}}{T'_{d0}} & -\frac{K_{qde}}{T'_{d0}} & \frac{K_{qb}}{T'_{d0}} & -\frac{K_{qdb}}{T'_{d0}} \\ \frac{K_A}{T_A} & -\frac{K_A K_{ve}}{T_A} & -\frac{K_A K_{vde}}{T_A} & -\frac{K_A K_{vb}}{T_A} & -\frac{K_A K_{vdb}}{T_A} \\ 0 & K_{ce} & K_{cde} & K_{cb} & K_{cdb} \end{bmatrix}$$

3.2.4 Determining different constants of linearized model

Now, it is very important to know the values of constant terms. From equation (3.2.15-3.2.22) we get the values for B constants.

$B_1 = -\frac{X_{dE} V_{b0} Sin\ \delta_0}{X_{d\Sigma}}$

$B_2 = \frac{X_{BB}}{X_{d\Sigma}}$

$B_3 = \frac{X_{dE} m_{B0} Sin\ \delta_{B0}}{2X_{d\Sigma}} - \frac{X_{Bd} m_{E0} Sin\ \delta_{E0}}{2X_{d\Sigma}}$

$B_4 = -\frac{X_{Bd} V_{dc0} Sin\ \delta_{E0}}{2X_{d\Sigma}}$

$B_5 = -\frac{\text{mE0}\ X_{Bd} V_{dc0} Cos\ \delta_{E0}}{2X_{d\Sigma}}$

$B_6 = \frac{X_{dE} V_{dc0} Sin\ \delta_{B0}}{2X_{d\Sigma}}$

$B_7 = \frac{\text{mB0}\ X_{dE} V_{dc0} Cos\ \delta_{B0}}{2X_{d\Sigma}}$

$B_8 = -\frac{X_{dt} V_{b0} Sin\ \delta_0}{X_{d\Sigma}}$

$B_9 = \frac{X_E}{X_{d\Sigma}}$

$B_{10} = \frac{X_{dE} m_{E0} Sin\ \delta_{E0}}{2X_{d\Sigma}} - \frac{X_{dt} m_{B0} Sin\ \delta_{B0}}{2X_{d\Sigma}}$

$B_{11} = -\frac{X_{dE} V_{dc0} Sin\ \delta_{E0}}{2X_{d\Sigma}}$

$B_{12} = \frac{\text{mE0}\ X_{dE} V_{dc0} Cos\ \delta_{E0}}{2X_{d\Sigma}}$

$B_{13} = -\frac{X_{dt} V_{dc0} Sin\ \delta_{B0}}{2X_{d\Sigma}}$

$B_{14} = -\frac{\text{mB0}\ X_{dt} V_{dc0} Cos\ \delta_{B0}}{2X_{d\Sigma}}$

$B_{15} = B_1 + B_8$

$B_{16} = B_2 + B_9$

$B_{17} = B_3 + B_{10}$

$B_{18} = B_4 + B_{11}$

$B_{19} = B_5 + B_{12}$

$B_{20} = B_6 + B_{13}$

$B_{21} = B_7 + B_{14}$

$B_{22} = -\frac{X_{qE} V_{b0} Cos\ \delta_0}{X_{q\Sigma}}$

$B_{23} = 0$

$B_{24} = \frac{X_{Bq} m_{E0} Cos\ \delta_{E0}}{2X_{q\Sigma}} - \frac{X_{qE} m_{B0} Cos\ \delta_{B0}}{2X_{q\Sigma}}$

$B_{25} = \frac{X_{Bq} V_{dc0} Cos\ \delta_{E0}}{2X_{q\Sigma}}$

$B_{26} = - \frac{\text{mE0}\ X_{Bq} V_{dc0} Sin\ \delta_{E0}}{2X_{q\Sigma}}$

$B_{27} = - \frac{X_{qE} V_{dc0} Cos\ \delta_{B0}}{2X_{q\Sigma}}$

$B_{28} = \frac{\text{mB0}\ X_{qE} V_{dc0} Sin\ \delta_{B0}}{2X_{q\Sigma}}$

$B_{29} = \frac{X_{qt} V_{b0} Cos\ \delta_0}{X_{q\Sigma}}$

$B_{30} = 0$

$B_{31} = \frac{X_{qt}\, m_{B0} Cos\ \delta_{B0}}{2X_{q\Sigma}} - \frac{X_{qE} m_{E0} Cos\ \delta_{E0}}{2X_{q\Sigma}}$

$B_{32} = - \frac{X_{qE} V_{dc0} Cos\ \delta_{E0}}{2X_{q\Sigma}}$

$B_{33} = \frac{\text{mE0}\ X_{qE} V_{dc0} Sin\ \delta_{E0}}{2X_{q\Sigma}}$

$B_{34} = \frac{X_{qt} V_{dc0} Cos\ \delta_{B0}}{2X_{q\Sigma}}$

$B_{35} = - \frac{\text{mB0}\ X_{qt} V_{dc0} Sin\ \delta_{B0}}{2X_{q\Sigma}}$

$B_{36} = B_{22} + B_{29}$

$B_{37} = B_{23} + B_{30}$

$B_{38} = B_{24} + B_{31}$

$B_{39} = B_{25} + B_{32}$

$B_{40} = B_{26} + B_{33}$

$B_{41} = B_{27} + B_{34}$

$B_{42} = B_{28} + B_{35}$

$B_{43} = X_q\ B_{36}$

$B_{44} = X_q\ B_{37}$

$B_{45} = X_q\ B_{38}$

$B_{46} = X_q\ B_{39}$

$B_{47} = X_q\ B_{40}$

$B_{48} = X_q\ B_{41}$

$B_{49} = X_q\ B_{42}$

$B_{50} = - X'_d\ B_{15}$

$B_{51} = (1 - X'_d)\ B_{16}$

$B_{52} = - X'_d\ B_{17}$

$B_{53} = - X'_d\ B_{18}$

$B_{54} = - X'_d\ B_{19}$

$B_{55} = - X'_d B_{20}$ $B_{56} = - X'_d B_{21}$

Now, to find out the values of K constants, we need to use the equations (3.2.23-3.2.26). All the K constants we have found are the functions of B constants.

$K_1 = V_{d0} B_{15} + i_{d0} B_{43} + V_{q0} B_{36} + i_{q0} B_{50}$

$K_2 = V_{d0} B_{16} + i_{d0} B_{44} + V_{q0} B_{37} + i_{q0} B_{51}$

$K_{pd} = V_{d0} B_{17} + i_{d0} B_{45} + V_{q0} B_{38} + i_{q0} B_{52}$

$K_{pe} = V_{d0} B_{18} + i_{d0} B_{46} + V_{q0} B_{39} + i_{q0} B_{53}$

$K_{pde} = V_{d0} B_{19} + i_{d0} B_{47} + V_{q0} B_{40} + i_{q0} B_{54}$

$K_{pb} = V_{d0} B_{20} + i_{d0} B_{48} + V_{q0} B_{41} + i_{q0} B_{55}$

$K_{pdb} = V_{d0} B_{21} + i_{d0} B_{49} + V_{q0} B_{42} + i_{q0} B_{56}$

$K_4 = (X'_d - X_d) B_{15}$ $K_3 = (X'_d - X_d) B_{16} - 1$

$K_{qd} = (X'_d - X_d) B_{17}$ $K_{qe} = (X'_d - X_d) B_{18}$

$K_{qde} = (X'_d - X_d) B_{19}$ $K_{qb} = (X'_d - X_d) B_{20}$

$K_{qdb} = (X'_d - X_d) B_{21}$ $K_5 = \frac{Vd0}{Vt0} B_{43} + \frac{Vq0}{Vt0} B_{50}$

$K_6 = \frac{Vd0}{Vt0} B_{44} + \frac{Vq0}{Vt0} B_{51}$ $K_{vd} = \frac{Vd0}{Vt0} B_{45} + \frac{Vq0}{Vt0} B_{52}$

$K_{ve} = \frac{Vd0}{Vt0} B_{46} + \frac{Vq0}{Vt0} B_{53}$ $K_{vde} = \frac{Vd0}{Vt0} B_{47} + \frac{Vq0}{Vt0} B_{54}$

$K_{vb} = \frac{Vd0}{Vt0} B_{48} + \frac{Vq0}{Vt0} B_{55}$ $K_{vdb} = \frac{Vd0}{Vt0} B_{49} + \frac{Vq0}{Vt0} B_{56}$

$K_7 = \frac{3}{4 C_{dc}} (m_{E0} \text{Cos}\delta_{E0} B_1 + m_{E0} \text{Sin}\delta_{E0} B_{22} + m_{B0} \text{Cos}\delta_{B0} B_8 + m_{B0} \text{Sin}\delta_{B0} B_{29})$

$K_8 = \frac{3}{4 C_{dc}} (m_{E0} \text{Cos}\delta_{E0} B_2 + m_{E0} \text{Sin}\delta_{E0} B_{23} + m_{B0} \text{Cos}\delta_{B0} B_9 + m_{B0} \text{Sin}\delta_{B0} B_{30})$

$K_9 = - \frac{3}{4 C_{dc}} (m_{E0} \text{Cos}\delta_{E0} B_3 + m_{E0} \text{Sin}\delta_{E0} B_{24} + m_{B0} \text{Cos}\delta_{B0} B_{10} + m_{B0} \text{Sin}\delta_{B0} B_{31})$

$K_{ce} = \frac{3}{4 C_{dc}} (m_{E0} \text{Cos}\delta_{E0} B_4 + m_{E0} \text{Sin}\delta_{E0} B_{25} + m_{B0} \text{Cos}\delta_{B0} B_{11} + m_{B0} \text{Sin}\delta_{B0} B_{32})$

$K_{cde} = \frac{3}{4 C_{dc}} (m_{E0} \text{Cos}\delta_{E0} B_5 - m_{E0} \text{Sin}\delta_{E0} B_{26} + m_{B0} \text{Cos}\delta_{B0} B_{12} + m_{B0} \text{Sin}\delta_{B0} B_{33})$

$K_{cb} = \frac{3}{4 C_{dc}} (m_{E0} \text{Cos}\delta_{E0} B_6 + m_{E0} \text{Sin}\delta_{E0} B_{27} + m_{B0} \text{Cos}\delta_{B0} B_{13} + m_{B0} \text{Sin}\delta_{B0} B_{34})$

$K_{cdb} = \frac{3}{4 C_{dc}} (m_{E0} \text{Cos}\delta_{E0} B_7 + m_{E0} \text{Sin}\delta_{E0} B_{28} + m_{B0} \text{Cos}\delta_{B0} B_{14} + m_{B0} \text{Sin}\delta_{B0} B_{35})$

Chapter 4

Design of Proportional Integral (PI) controller and Power System Stabilizer (PSS) for UPFC

4.1 Introduction to PI controller and PSS

The dynamic behavior of the power system model installed with UPFC, presented in chapter 3 has been investigated in this chapter for different PI controllers and PSS used. A basic feedback system of PI controller is given in Fig.4.1

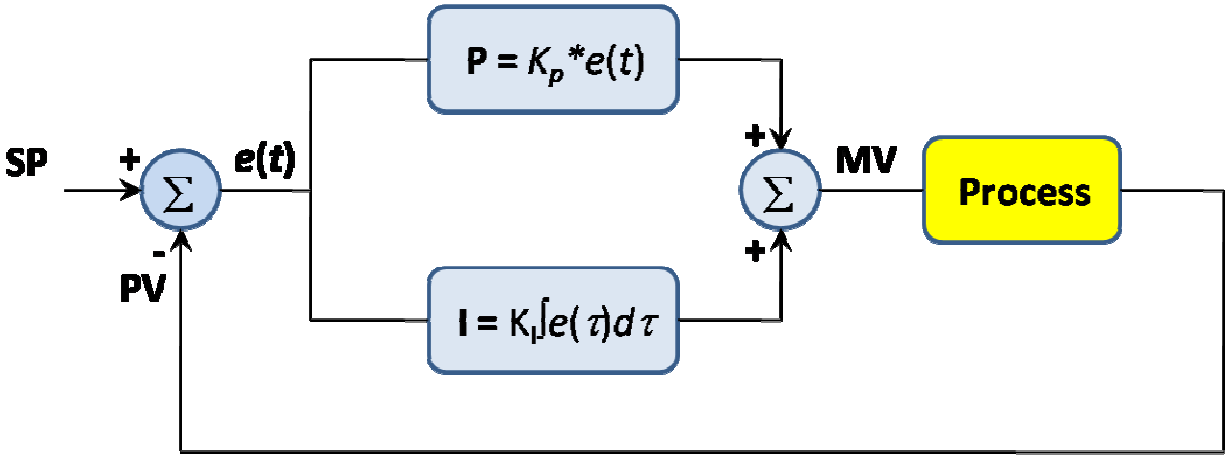

Figure 4.1: A basic feedback system with PI controller

The transfer function of a PI controller is $Gc(s) = K_p + \frac{K_I}{S}$

Where, K_p = Proportional gain, K_I =Integral gain

The variable e represents the tracking error, the difference between the desired input value R and the actual output Y. This error signal is fed to controller, and the output of the controller is given as $u = K_p e + K_I \int e dt$

The proportional controller K_p will affect the steady state error as well as rise time. An integral control K_I controls the transient response and the steady state error. The effect of each of controllers K_p an K_I on a closed-loop system are summarized in Table 4.1.

Close Loop Response	**Rise Time**	**Overshoot**	**Settling Time**	**Steady State Error**
K_p	Decrease	Increase	Small change	Decrease
K_I	Decrease	Increase	Increase	Eliminate

Table 4.1: Characteristics of PI controller in close loop system

There is a degree of dependence of K_p and K_I on each other. In fact, changing one of these variables K_p and K_I can change the effect of the other. For this reason, the table should only be used as a reference for choosing of K_p and K_I.

In section 3.1.2, it has already been discussed about power system stabilizer (PSS). In general, need of PSS is felt in situations when power has to be transmitted over long distances with weak AC ties. Even when PSS may not be required under normal operating conditions, they allow satisfactory operation under unusual or abnormal conditions which may be encountered at times. Thus, PSS has become a standard option with modern static exciters and it is essential for power engineers to use these effectively. Retrofitting of existing excitation systems with PSS may also be required to improve power system stability.

The instability arises due to the negative damping torque caused by fast acting exciter. The objective and work of PSS is to introduce additional damping torque without affecting the synchronizing torque. The obvious control signal (to be used as input to the PSS) is the deviation

in the rotor velocity. However, for practical implimentation, other signals such as bus frequency. Electrical power, accelerating power are also used.

4.2 Updated model of SMIB with PI controller and PSS

In the figure 4.2, we have got one lead-lag controller (PSS) connected to UPFC. Δw is the input to the system block. Let us consider Δy_1 after multiplying with $\frac{KsT_w}{1+sT_w}$, Δy_2 after $\frac{1+sT_1}{1+sT_2}$ and ΔC after $\frac{1+sT_3}{1+sT_4}$ as the input to the summing junction. ΔU_{ref} is the another input to the junction. Output of junction (ΔCa), after passing through block $\frac{Ks}{1+sT_s}$, gives output Δu finally.

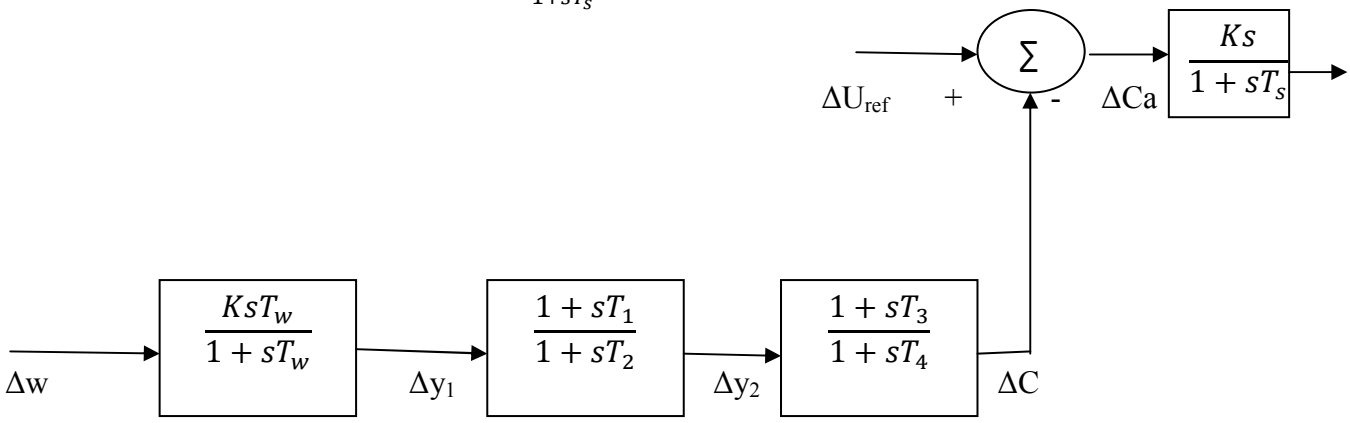

Fig 4.2: Lead-lag controller connected UPFC

This Δu is infact the control signal of UPFC which can be any one of the four signals m_E, m_B, δ_E, and δ_B. If Δm_B is chosen as Δu, then the ΔU_{ref} will be $\Delta m_{B\,ref}$. So, like this way reference signals are selected depending upon the value of Δu.

So, we can write, $\frac{\Delta y1}{\Delta w} = \frac{KsT_w}{1+sT_w}$

$$\Rightarrow \Delta y_1 + \Delta \dot{y}_1 \, Tw = K \, \Delta \dot{w} \, Tw$$

$$\Rightarrow \Delta \dot{y}_1 = [K \, \Delta \dot{w} \, Tw - \Delta y_1] \frac{1}{T_w} \qquad (4.1)$$

Again, $\frac{\Delta y2}{\Delta y1} = \frac{1+sT_1}{1+sT_2}$

$$\Rightarrow \Delta y_2 + \Delta \dot{y}_2 T_2 = \Delta y_1 + \Delta \dot{y}_1 T_1$$

$$\Rightarrow \Delta \dot{y}_2 = [\Delta y_1 + \Delta \dot{y}_1 T_1 - \Delta y_2] \frac{1}{T_2} \quad (4.2)$$

And $\frac{\Delta C}{\Delta y2} = \frac{1+sT_3}{1+sT_4}$

$$\Rightarrow \Delta C + \Delta \dot{c}\, T_4 = \Delta y_2 + \Delta \dot{y}_2 T_3$$

$$\Rightarrow \Delta \dot{c} = [-\Delta C + \Delta \dot{\delta}_E T_3 + \Delta y_2] \frac{1}{T_4} \quad (4.3)$$

Now, introducing PI controller block with previous block diagram gives a figure like this:

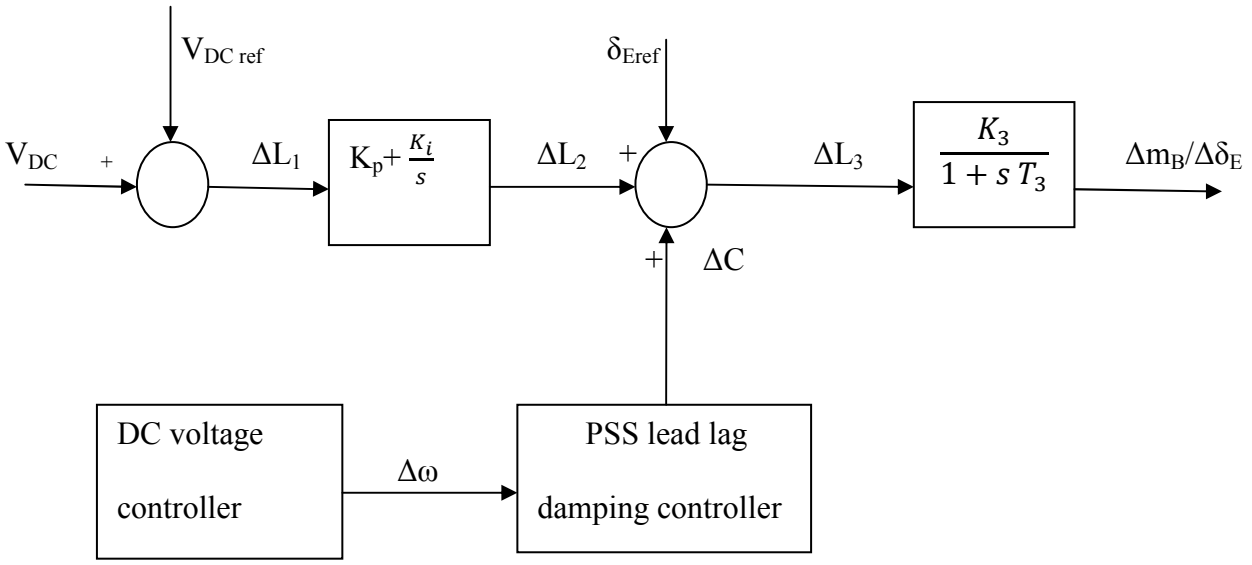

Figure 4.3 UPFC with lead-lag controller and DC voltage regulator

Let us think ΔL_1 as the output of 1st summing junction. ΔL_2 is the output from PI controller block. ΔL_3 is the output of the junction summing up ΔL_2, δ_{Eref} and the output of PSS, ΔC.

$\Delta L_1 = V_{Dcref} - V_{DC}$

$\frac{\Delta L2}{\Delta L1} = K_p + \frac{K_i}{s} = \frac{K_p s + K_i}{s}$

$\Rightarrow \quad \Delta \dot{L}_2 = K_p \Delta \dot{L}_1 + K_i \Delta L_1 \qquad (4.4)$

$\Delta L_3 = \Delta L_2 + \Delta C + \delta_{Eref}$

$\frac{\Delta \delta E}{\Delta L3} = \frac{K_3}{1 + s T_3}$

$\Rightarrow \quad \Delta \delta_E + \Delta \dot{\delta}_E T_3 = K_s \Delta L_3$

$\Rightarrow \quad \Delta \dot{\delta}_E = [K_s \Delta L_3 - \Delta \delta_E] \frac{1}{T_s} \qquad (4.5)$

So, we have got five new state equations (4.1-4.5) which will be added with the system model of UPFC connected SMIB derived in chapter 3.

4.3 Effect of only PSS on SMIB system model

After doing the complete modeling (linear and nonlinear) of UPFC connected power system, response curves are observed in this chapter. All the system responses observed in this chapter are for 10 seconds. The values for different parameters which are used in modeling are listed in appendix B & C in detail.

Pe=0.8 & Qe=0.1670 is the loading values which are used here. This has been treated as nominal loading while light and heavy loading responses are being discussed in chapter 5. Response is observed first without giving the system any kind of disturbances. As there is no disturbance

present in the system, no oscillation will be seen in the output response. So, without disturbance, ΔV_{DC} vs. t curve looks like a straight line as in fig 4.4.

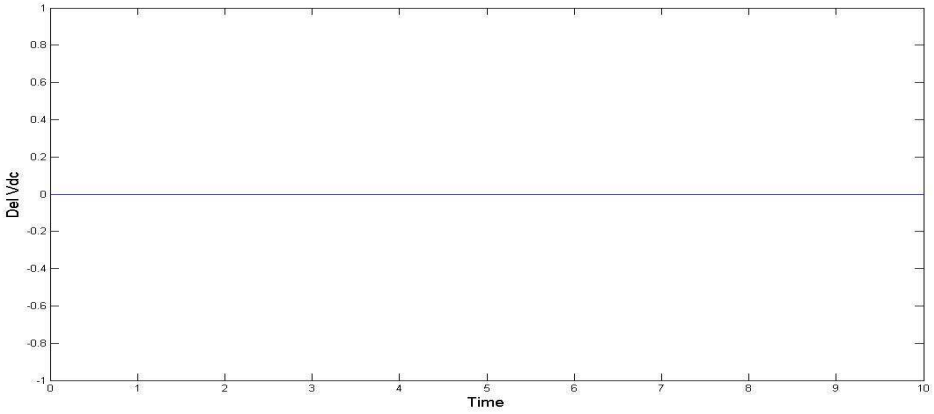

Fig 4.4: ΔV_{DC} vs. t curve for SMIB system without any disturbance

Then a pulse type disturbance of amplitude 1pu is added with the system which starts at 1s and ends in 1.1 secs. So, the duration of the disturbance is 0.1 second. The response of the system after being subjected with given disturbance (both +ve & -ve) is shown below in fig. 4.5. From this figure, a complete unstable situation of plant model is observed.

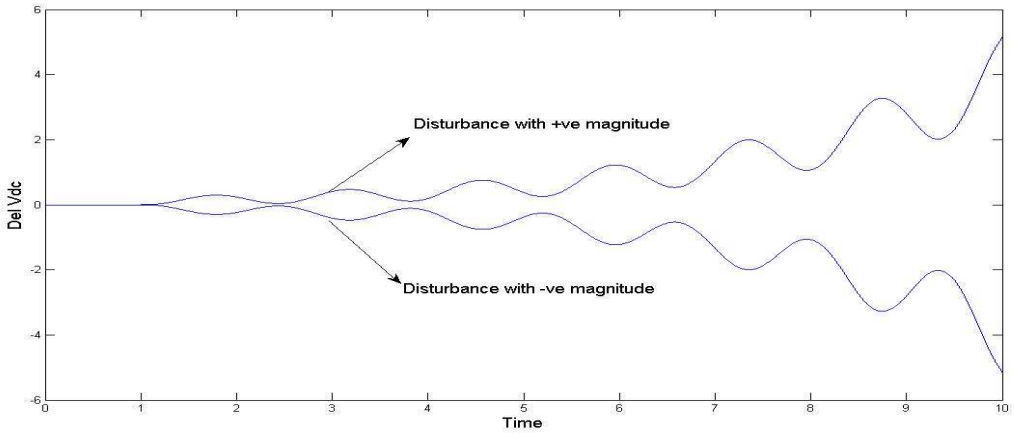

Fig. 4.5: ΔV_{DC} vs. t curve for SMIB system with a disturbance

To damp out this created oscillations, Power System Stabilizer (PSS) has been added now with the system. Effect of PSS on UPFC connected SMIB system model (fig 4.2) is shown in figure 4.6 for all the four control signals of UPFC: m_E, m_B, δ_E, and δ_B simultaneously.

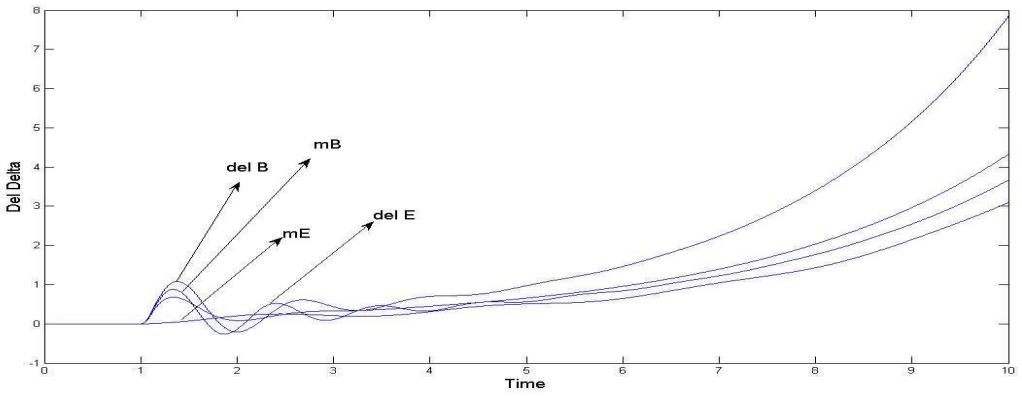

Fig 4.6: Δδ vs. t output curves of PSS connected SMIB system for all the control signals of UPFC

It has been found that all the control signals can reduce the oscillations but ultimately exponential rise in Δδ ensures system instability.

So it is needed to add a PI controller along with PSS which will help to make the system stable. In the next section (chapter 4.4), system responses are observed for all the five states (Δδ, Δω, $\Delta E'_q$, ΔE_{fd}, ΔV_{DC}) when both PSS and PI controller are connected with SMIB. Effect of different control signals (m_E, m_B, δ_E, and δ_B) are also shown for each of the case.

4.4 Combined effect of PSS and PI controller on different states of model

4.4.1 Effect on state ΔV_{dc}

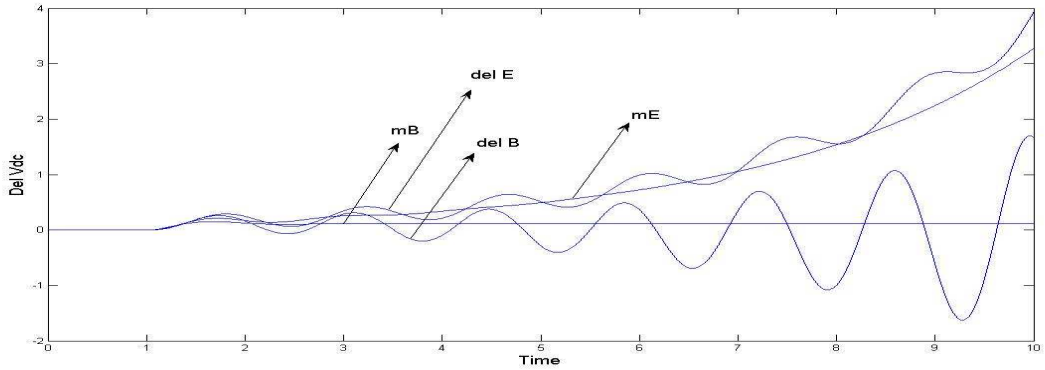

Fig 4.7: ΔV_{dc} Vs. time output curve of PSS and PI connected SMIB system for all the control signals

It has been found that (Fig 4.7) the control signals m_E, δ_E, and δ_B can't make the system stable. Only the control signal m_B have damped out the oscillations at 3.8 seconds while maximum peak of the response is 0.15pu.

It has been found that, among the four control signals, m_B and δ_E show better performance in system stability analysis than the other two. So, for the rest of the states, impact for these two control signals are only being observed.

4.4.2 Effect on state Δδ

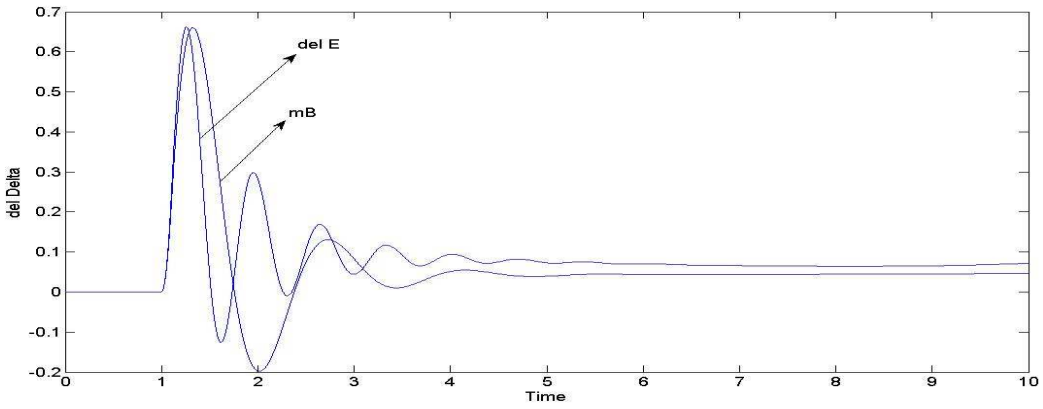

Fig 4.8: Δδ vs. time output curve of PSS and PI connected SMIB system for control signals m_B and δ_E

It has been found that (Fig 4.8) both m_B and δ_E provide stable output to the system response. m_B controlled response has the highest peak of 0.65pu and settling time is around 6 seconds. δ_E controlled response become stable at around 7 seconds with a maximum peak of 0.65pu.

4.4.3 Effect on state Δω

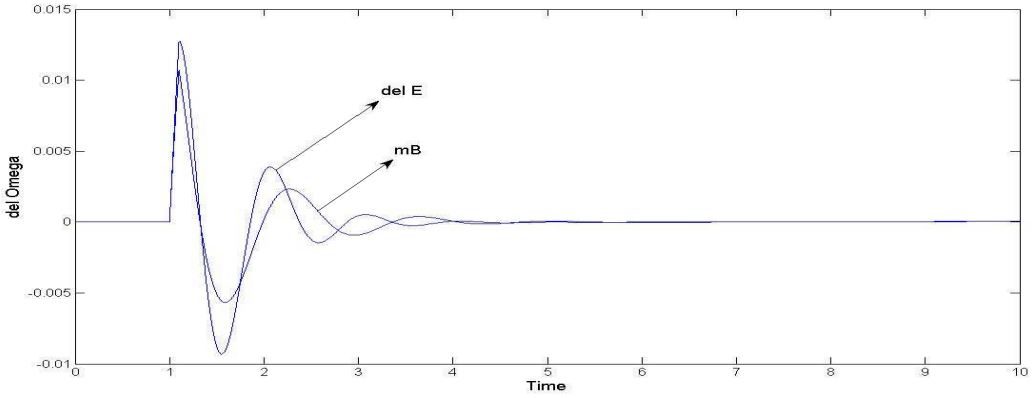

Fig 4.9: Δω Vs. time output curve of PSS and PI connected SMIB system for control signals m_B and δ_E

It has been found that (Fig 4.9) both m_B and δ_E provide stable output to the system response. m_B allows the response to rise upto a peak of 0.01pu which has the settling time of 5 seconds. δ_E controlled response become stable at around 7 seconds with a maximum peak of 0.013pu.

4.4.4 Effect on state $\Delta E'_q$

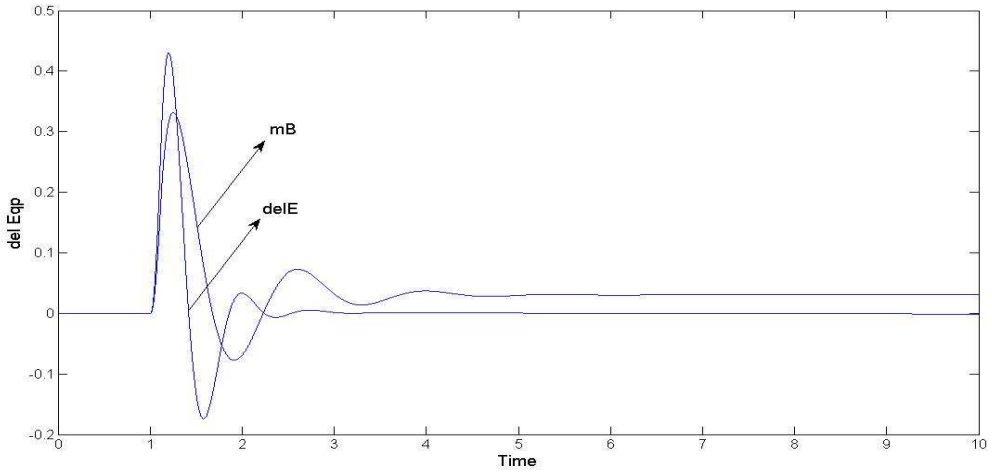

Fig 4.10: $\Delta E'_q$ Vs. time output curve of PSS and PI connected SMIB system for control signals m_B and δ_E

It has been found that (Fig 4.10) both m_B and δ_E provide stable output to the system response. m_B controlled response has the highest peak of 0.32pu and settling time is around 6.2 seconds. δ_E controlled response become stable at around 3.4 seconds with a maximum peak of 0.42pu.

4.4.5 Effect on state ΔE_{fd}

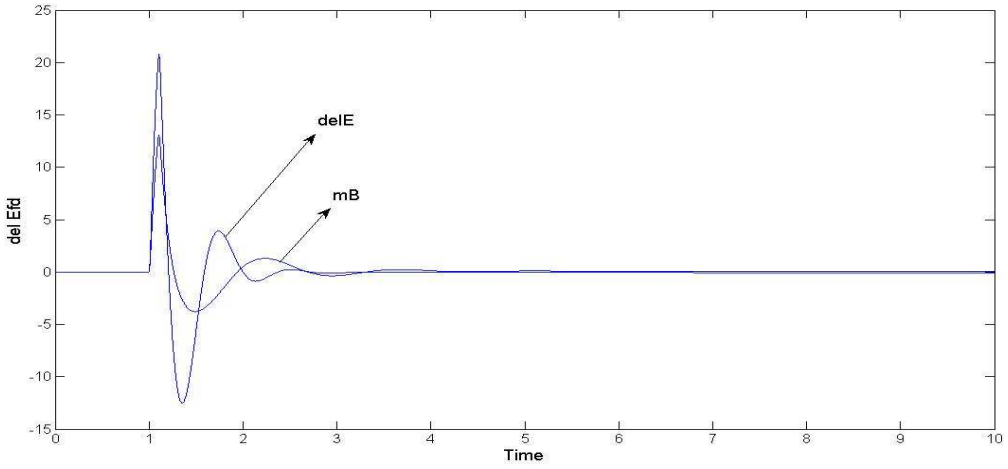

Fig 4.11: ΔE_{fd} Vs. time output curve of PSS and PI connected SMIB system for control signals m_B and δ_E

It has been found that (Fig 4.11) both m_B and δ_E provide stable output to the system response. m_B allows the response to rise upto a peak of 12pu which has the settling time of 4 seconds. δ_E controlled response become stable at around 4 seconds with a maximum peak of 21pu.

Chapter 5

Analysis for different loading conditions and Eigen Value analysis of stability

5.1 Analysis for three different loading conditions on different states

The analysis shown in chapter 4 is done for a loading of Pe=0.8 & Qe=0.1670. In this chapter, response for two more loading types is observed. One is heavy loading (Pe=1.2 & Qe=0.4) and another is light loading (Pe=0.2 & Qe=0.01). Table of information about different loading conditions is given in appendix D.

5.1.1 Heavy loading condition

5.1.1.1 Effect for PSS only

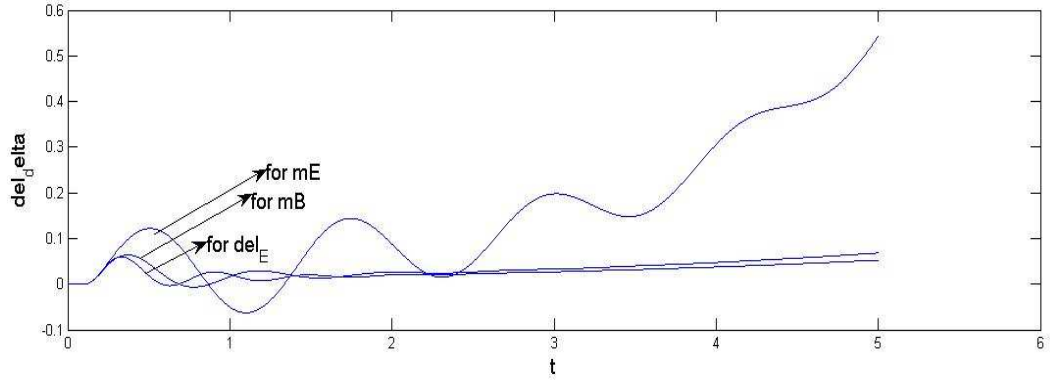

Fig 5.1: $\Delta\delta$ Vs. time output curve of PSS connected SMIB system for control signals $m_{E,}$ m_B and δ_E (heavy loading)

It has been found that (Fig 5.1) none of the control signals can make the system stable completely. m_B & δ_E gives better response damping out the oscillations but cant't make it stable.

5.1.1.2 Effect on state ΔV_{dc} for both PSS & PI controller

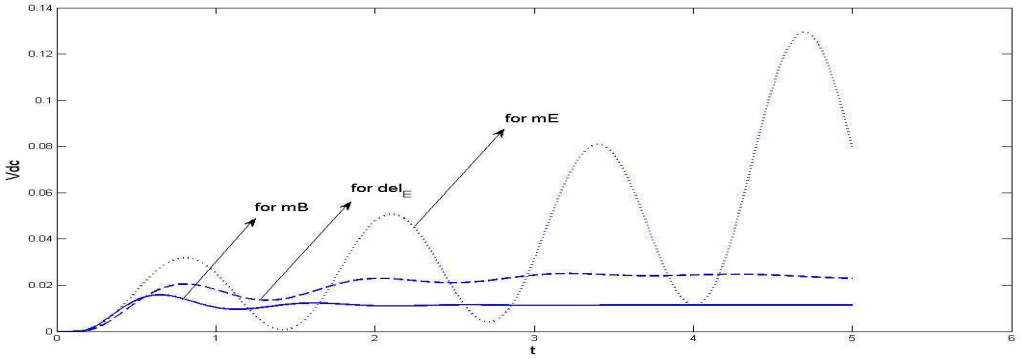

Fig 5.2: ΔV_{DC} Vs. time output curve of PSS & PI connected SMIB system for control signals m_E, m_B and δ_E (heavy loading)

It has been found that (Fig 5.2) control signal m_B gives the best response making the system stable. δ_E has a better response than m_E but none of them can bring stability in the system.

5.1.1.3 Effect on state $\Delta\delta$ for both PSS & PI controller

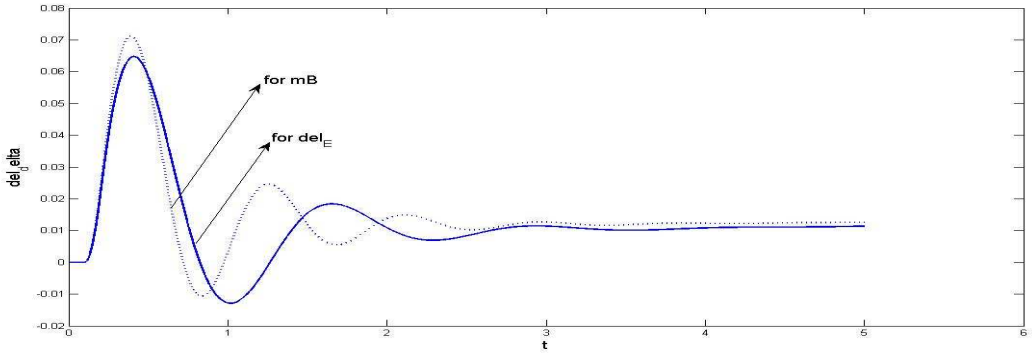

Fig 5.3: $\Delta\delta$ Vs. time output curve of PSS & PI connected SMIB system for control signals m_B and δ_E (heavy loading)

It has been seen that (Fig 5.3) both m_B and δ_E provide stable operation as system response.

5.1.1.4 Effect on state Δω for both PSS & PI controller

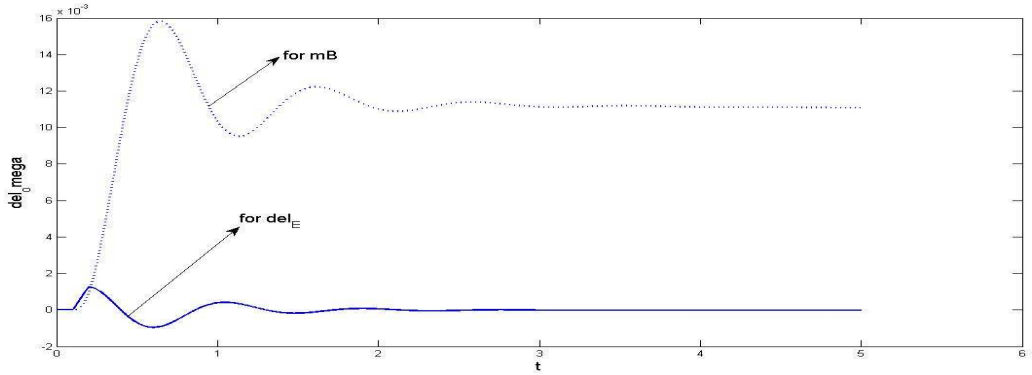

Fig 5.4: Δω Vs. time output curve of PSS & PI connected SMIB system for control signals m_B and δ_E (heavy loading)

It has been found that (Fig 5.4) both m_B and δ_E provide stable output to the system response as we found for nominal loading.

5.1.2 Light loading condition

5.1.2.1 Effect for PSS only

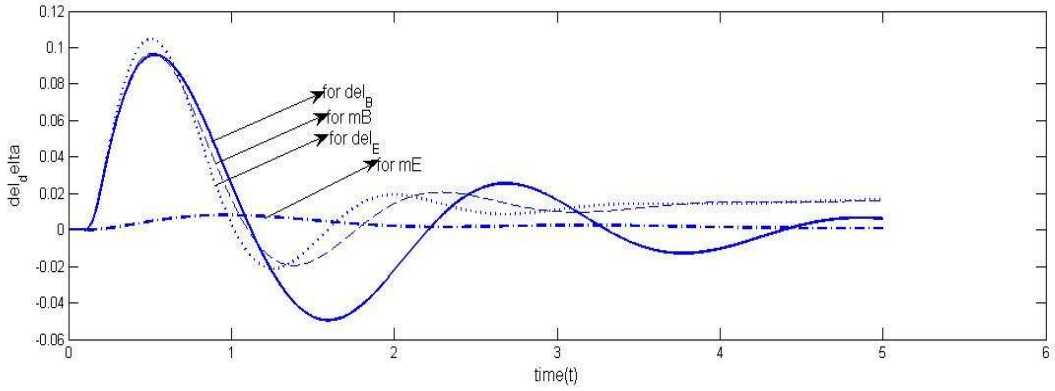

Fig 5.5: Δδ Vs. time output curve of PSS connected SMIB system for control signals m_E, δ_B, m_B and δ_E (light loading)

It has been seen that (Fig 5.5) only the control signal m_E can give a stable operation. m_B and δ_E gives a good response but can't make the system stable completely. δ_B has the worst response.

5.1.2.2 Effect on state ΔV_{dc} for both PSS & PI controller

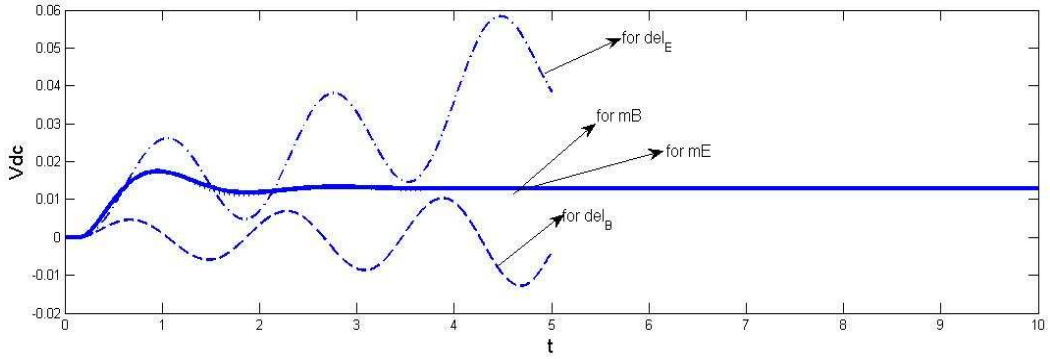

Fig 5.6: ΔV_{DC} Vs. time output curve of PSS & PI connected SMIB system for control signals m_E, δ_B, m_B and δ_E (light loading)

It has been found that (Fig 5.6) both m_B and m_E provide stable output to the system response where δ_B and δ_E can't.

5.1.2.3 Effect on state $\Delta\delta$ for both PSS & PI controller

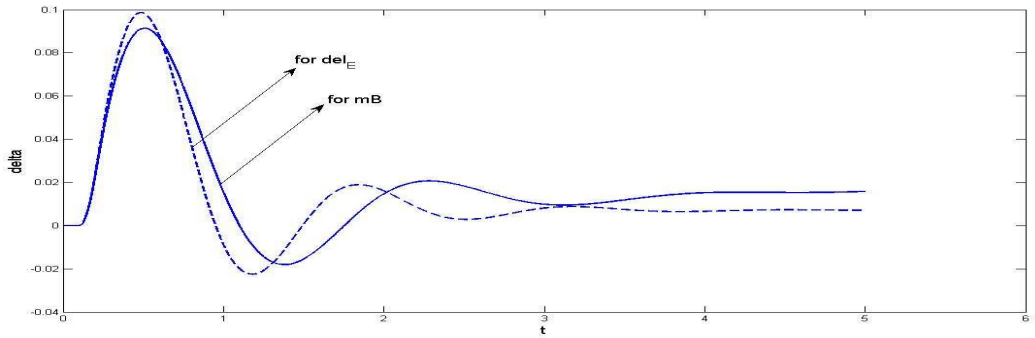

Fig 5.7: $\Delta\delta$ Vs. time output curve of PSS & PI connected SMIB system for control signals m_B and δ_E (light loading)

It has been found that (Fig 5.7) both m_B and m_E provide stable output to the system response where δ_B and δ_E can't.

5.1.2.4 Effect on state Δω for both PSS & PI controller

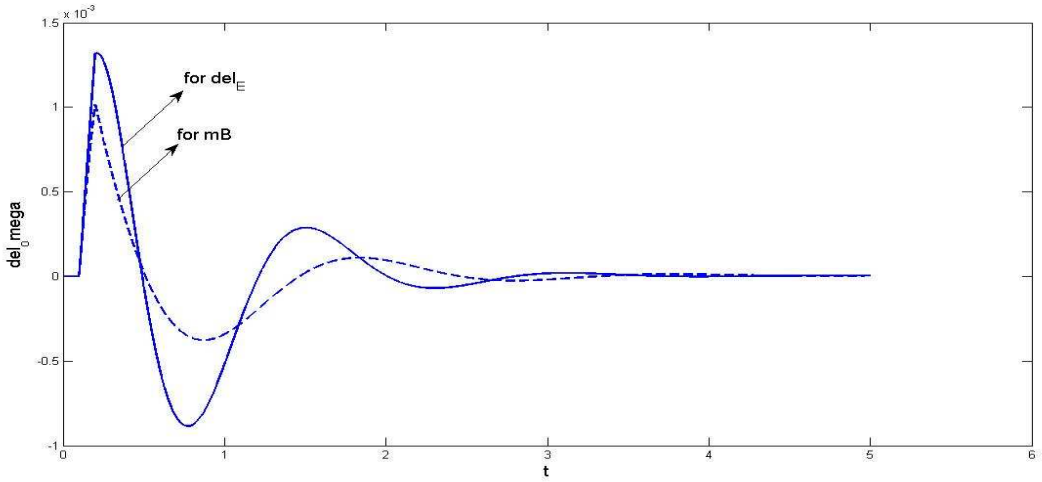

Fig 5.8: Δω Vs. time output curve of PSS & PI connected SMIB system for control signals m_B and δ_E (light loading)

It has been found that (Fig 5.8) both m_B and m_E provide stable output to the system response where δ_B and δ_E can't.

5.2 Eigen value analysis for stability

In the previous two chapters, stability analysis is done by seeing the output response of the system. Stability can also be checked by seeing the Eigen value of the system matrix derived from the system model. Stability behavior of the system model from Eigen value analysis is like this:

- **The Eigen values are real numbers.**

1. Eigen values both positive

Unstable: All trajectories in the neighborhood of the fixed point will be directed outwards and away from the fixed point.

2. Eigen values both negative

Stable: All trajectories in the neighborhood of the fixed point will be directed towards the fixed point.

3. Eigen values opposite sign

Unstable: Trajectories in the general direction of the negative eigen value's eigenvector will initially approach the fixed point but will diverge as they approach a region dominated by the positive (unstable) eigen value.

- **Eigen values are complex conjugates**

1. Real parts positive

Unstable: All trajectories in the neighborhood of the fixed point spiral away from the fixed point with ever increasing radius.

2. Real parts negative

Stable: All trajectories in the neighborhood of the fixed point spiral into the fixed point with ever decreasing radius.

Eigen values with “bold” numbers in following tables indicate the unstable condition of system.

Table 5.1: System Eigen values of nominal loading for different control signals and with no controller

PSS+PI				Only PSS		No controller
δ_E	δ_B	m_B	m_E	m_B	δ_E	
-0.0100	-9.9983	-9.9718	-9.9682	-9.9778	-0.0100	-92.7141
-1.0021	-0.9273	-0.9320	-0.9298	-0.9314	-1.0007	-7.4346
-0.0938	-0.0731	-0.0749 +	-0.0865 +	-0.0605 +	-0.0931	**0.0146 +**
-0.0010	**0.0023 +**	0.0421i	0.0415i	0.0375i	-0.0009 +	**4.4536i**
+0.0095i	**0.0450i**	-0.0749 -	-0.0865 -	-0.0605 -	0.0062i	**0.0146 -**
-0.0010	**0.0023 -**	0.0421i	0.0415i	0.0375i	-0.0009 -	**4.4536i**
- 0.0095i	**0.0450i**	-0.0212 +	-0.0125 +	-0.0245 +	0.0062i	**0.5286**
-0.0018	-0.0048	0.0400i	0.0385i	0.0411i	0.0003	
0.0004	**0.0006 +**	-0.0212 -	-0.0125 -	-0.0245 -	-0.0001	
-0.0001+	**0.0029i**	0.0400i	0.0385i	0.0411i	-0.0039	
0.0000i	**0.0006 -**	0.0003	**0.0033**	**0.0034**	-0.0100	
-0.0001 -	**0.0029i**	-0.0010	-0.0010	-0.0053		
0.0000i	-0.0010	-0.0333	-0.0333	-0.0333		
-0.0100	-0.0500	-0.0000	0.0000			

Table 5.2: System Eigen values of heavy loading for different control signals and with no controller

PSS+PI				Only PSS		No controller
m_B	δ_E	δ_B	m_E	m_B	δ_E	
-9.9803	-0.0100	-1.0211	-9.9915	-1.0032	-0.0100	-93.1600
-0.9376	-1.0007	-0.0932	-0.9350	-0.0949	-1.0001	-7.7296
-0.0688	-0.0934	**0.0202**	-0.0784 +	-0.0014 +	-0.0939	**0.3844 +**
+0.0444i	-0.0015 +	-0.0077	0.0339i	0.0115i	-0.0014 +	**4.8713i**
-0.0688	0.0078i	**0.0011 +**	-0.0784 -	-0.0014 -	0.0083i	**0.3844 -**
- 0.0444i	-0.0015 -	**0.0018i**	0.0339i	0.0115i	-0.0014 -	**4.8713i**
-0.0204	0.0078i	**0.0011 -**	-0.0064 +	-0.0035 +	0.0083i	**0.5300**
+0.0482i	-0.0024	**0.0018i**	0.0502i	0.0010i	-0.0029	
-0.0204	0.0002	-0.0001 +	-0.0064 -	-0.0035 -	0.0003	
- 0.0482i	-0.0000	0.0001i	0.0502i	0.0010i	-0.0001	
0.0004	-0.0001	-0.0001 -	**0.0034**	0.0003	-0.0100	
-0.0010	-0.0100	0.0001i	-0.0010	-0.0001		
-0.0333		-0.0000	-0.0333	-0.0033		
-0.0000		-0.0050	0.0000			

Table 5.3: System Eigen values of light loading for different control signals and with no controller

PSS+PI				Only PSS		No controller
m_B	δ_E	δ_B	m_E	m_B	δ_E	
-9.9943	-0.0100	-1.0064	-1.0000	-9.9991	-0.0100	-92.0300
-0.9243	-1.0007	-0.0921	-0.0927	-0.9240	-1.0008	-7.4735
-0.0727 +0.0336i	-0.0924	-0.0072 -0.0015 + 0.0052i	-0.0059 + 0.0049i	-0.0606 + 0.0321i	-0.0924 -0.0017 + 0.0048i	-0.0993 + 3.6103i
-0.0727 - 0.0336i	-0.0015 + 0.0052i	**0.0048 + 0.0022i**	-0.0059 - 0.0049i	-0.0606 - 0.0321i	-0.0017 - 0.0048i	-0.0993 - 3.6103i
-0.0148 +0.0354i	-0.0015 - 0.0052i	**0.0008 - 0.0022i**	-0.0024 + 0.0032i	-0.0161 + 0.0355i	-0.0019 + 0.0003i	**0.1666**
-0.0148 - 0.0354i	-0.0032	-0.0005	-0.0024 - 0.0032i	-0.0161 - 0.0355i	-0.0019 - 0.0003i	
0.0001	0.0002	-0.0001	0.0001	-0.0054		
-0.0010	-0.0001	-0.0001	-0.0001	0.0011	0.0001	
-0.0333	-0.0002	-0.0050	-0.0033	-0.0333	-0.0100	
- 0.0000	-0.0100		-0.0000			

Chapter 6

Effect of Model Predictive Controller (MPC) for UPFC connected SMIB

6.1 Introduction about MPC

6.1.1 Basic Working Principle:

Model predictive control (MPC) refers to a class of computer control algorithms that utilize an explicit process model to predict the future response of a plant. At each control interval an MPC algorithm attempts to optimize future plant behavior by computing a sequence of future manipulated variable adjustments. The first input in the optimal sequence is then sent into the plant, and the entire calculation is repeated at subsequent control intervals. Originally developed to meet the specialized control needs of power plants and petroleum refineries, MPC technology can now be found in a wide variety of application areas including chemicals, food processing, automotive, and aerospace applications [55, 56].

The working process of MPC can be well described by the chess play. A player, when plays chess, tries to predict the future moves of the opponent. So, to win the match, he predicts about some future moves depending upon his past experiences and memories. A good player has always got some plans about his next moves or actions.

Figure 6.1 shows the basic structure of MPC in block diagrams. Depending upon the past inputs and outputs, model predicts the future output. It is compared with reference value and the subtracted result or future error is sent to the optimizer. With the help of quadratic cost function

and suitable constraints, it creates the future inputs of the optimizer which is actually the past memory of the model. Thus it creates a loop and the circle continues until it reaches close to the desired reference value.

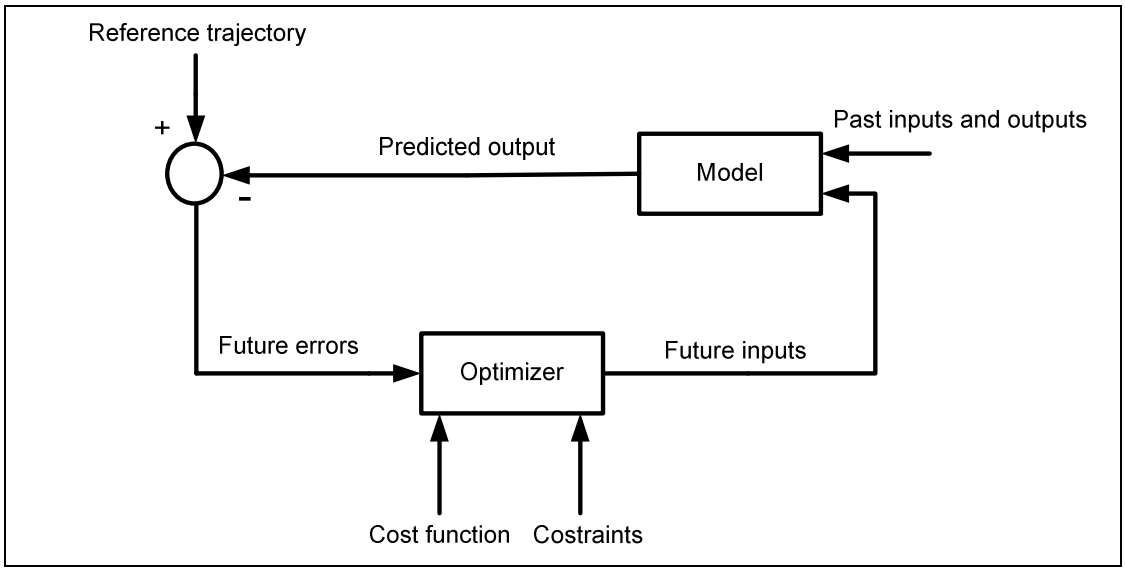

Figure 6.1: Basic structure of MPC

A model is used to predict the future plant outputs based on past and current values and the proposed optimal future control actions. These actions are calculated by the optimizer taking into account the cost function (where the future tracking error is considered) as well as the constraints [57].

That means the set of future control signals is calculated by optimizing a determined criterion in order to keep the process as close as possible to the reference trajectory. This criterion usually takes the form of a quadratic function of the errors between the predicted output signal and the predicted reference trajectory. The control effort is included in the objective function in most cases.

The process model plays here the decisive role in the controller. The chosen model must be capable of capturing the process dynamics so as to precisely predict the future outputs as well as being simple to implement and to understand. As MPC is not an unique technique but a combination of different methodologies, there are many types of models used in various formulations like Truncated Impulse Response Model, Transfer Function Model, Step Response Model etc [58].

6.1.2 A Brief History of Industrial MPC:

Rawlings [56] provides an excellent introductory tutorial aimed at control practitioners. Allgower, Badgwell, Qin, Rawlings, and Wright [59] present a more comprehensive overview of nonlinear MPC and moving horizon estimation, including a summary of recent theoretical developments and numerical solution techniques. Mayne, Rawlings, Rao, and Scokaert [60] provide a comprehensive review of theoretical results on the closed-loop behavior of MPC algorithms. The authors presented a survey of industrial MPC technology based on linear models at the 1996 Chemical Process Control V Conference (Qin & Badgwell [61]), summarizing applications through 1995. Young, Bartusiak, and Fontaine [62], Downs [63], and Hillestad and Andersen [64] report development of MPC technology within operating companies. A survey of MPC technology in Japan provides a wealth of information on application issues from the point of view of MPC users (Ohshima, Ohno, & Hashimoto [65]). The first description of MPC control applications was presented by Richalet et al. in 1976 Conference (Richalet et al. [66]) and later summarized at 1978 in Automatica paper (Richalet et al. [67]). They described their approach as model predictive heuristic control (MPHC).

6.2: The "Reciding Horizon" Idea:

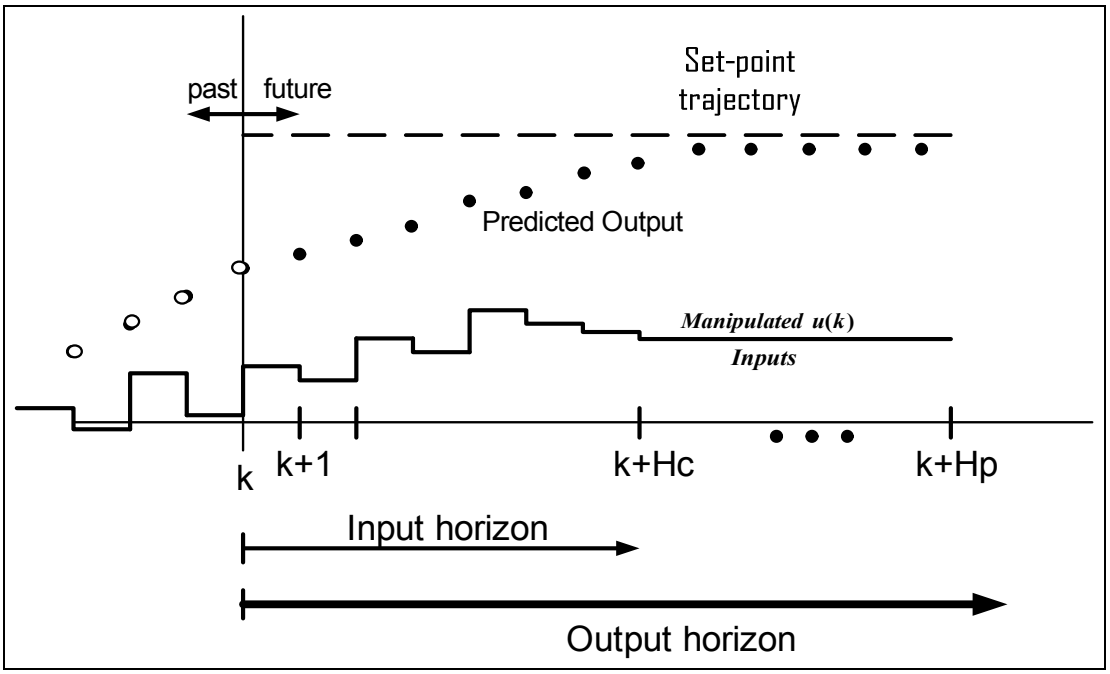

Figure 6.2: The receding horizon concept showing Optimization Problem

At a current instant k, the MPC solves an optimization problem over a finite prediction horizon $[k, k+H_P]$ with respect to a predetermined objective function such that the predicted state variable $\hat{x}$ or output $\hat{y}$ can optimally stay close to a reference trajectory. The control is computed over a control horizon $[k, k+H_C]$, which is smaller than the prediction horizon ($H_C \leq H_P$). If there were no disturbances, no model-plant mismatch and the prediction horizon is infinite, one could apply the control strategy found at current time k for all times. However, due to the disturbances, model-plant mismatch and finite prediction horizon, the true system behavior

is different from the predicted behavior. In order to incorporate the feedback information about the true system state, the computed optimal control is implemented only until the next measurement instant $(k, k+1)$, at which point the entire computation is repeated [58].

MPC approach can be expressed considering the following finite horizon cost function [68]

$$J^{rh}(x_t, [u_0(t), \ldots, u_{H-1}(t)]) = \sum_{i=1}^{H-1} h(\overline{x}_{t+i\Delta T}(u), u_i(t)) + g(\overline{x}_{t+H\Delta T}(u))$$

where t is the current time; H is the length of the optimization horizon; ΔT is the sample period. If i > 0, then $\overline{x}_{t+i\Delta T}(u)$ denotes the controlled trajectory at time $t+i\Delta T$ from x_t under piecewise controls $u = [u_0(t), ..., u_{i-1}(t)] \in U^H$; h is the running cost; and g is the terminal cost. We assume that h is non-negative function and g satisfies $g(x) \geq \alpha |x - x_{eq}|$ for all x, where x_{eq} is some desired equilibrium and α>0 is some positive constant. That is, g is an 'upward' function whose lowest point is at the system equilibrium. This condition on g(.) ensures that the control design attempts to reach the system equilibrium.

6.3 The UPFC connected SMIB Model controlled by MPC:

The output voltage of the voltage source converter can be regulated by applying appropriate triggering pulses. The block diagram of MPC and SMIB (connected with UPFC) is shown in Fig. 6.3. The MPC takes the error in the output and the matrices A and B from the linearized power system model with UPFC.

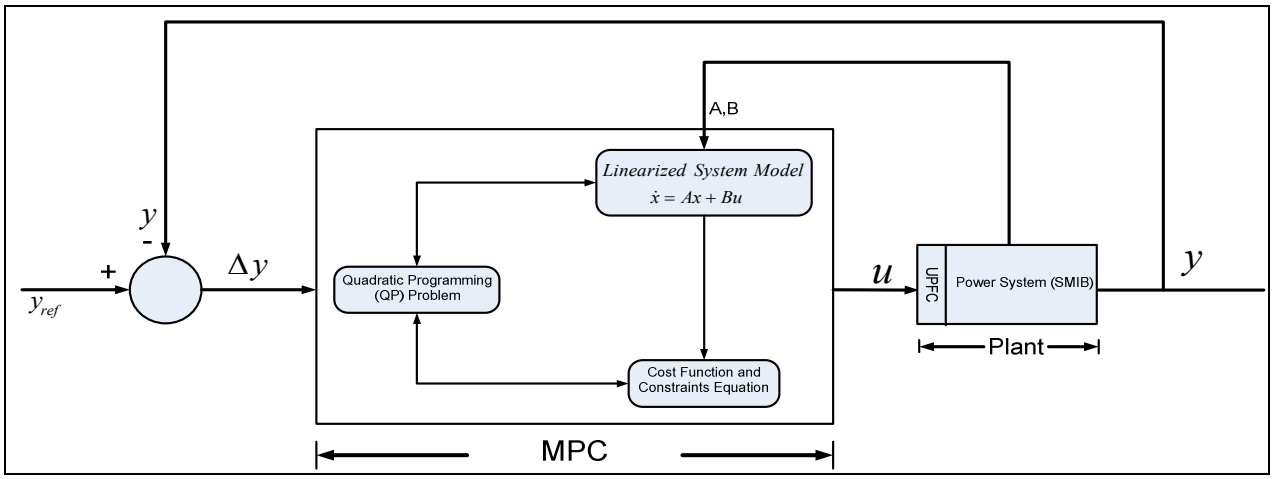

Figure 6.3: Block diagram representation of UPFC connected SMIB system controlled with MPC

Figure 6.4 shows the schematic overview of the overall plant model. The UPFC connected SMIB power system plant is connected here with the MPC block. The output of the plant (y) enters into the summing junction where it has been compared with the reference value (y_{ref}). Subtracted result (Δy) goes into the MPC block. The information about the plant (system matrix A,B) are already given to the MPC block. So, the linearized system model of the plant gives the future output (u) with the help of Quadratic Programming (QP) function of MPC and proper constraints of the MPC block. Predicted output of the controller, u enters into the plant and creates the next result y′. Thus the loop will continue until it reaches the desired reference trajectory of the plant.

Figure 6.4 show the circuital representation of UPFC connected SMIB system controlled with MPC which is actually the modification of Fig. 3.4. Working procedure of MPC in the proposed model can be described as the same way it has been described for figure 6.3.

Four control signals of UPFC (m_E, m_B, δ_E, and δ_B) are entering into the UPFC connected SMIB plant through MPC. Thus MPC is connected with the system model through UPFC.

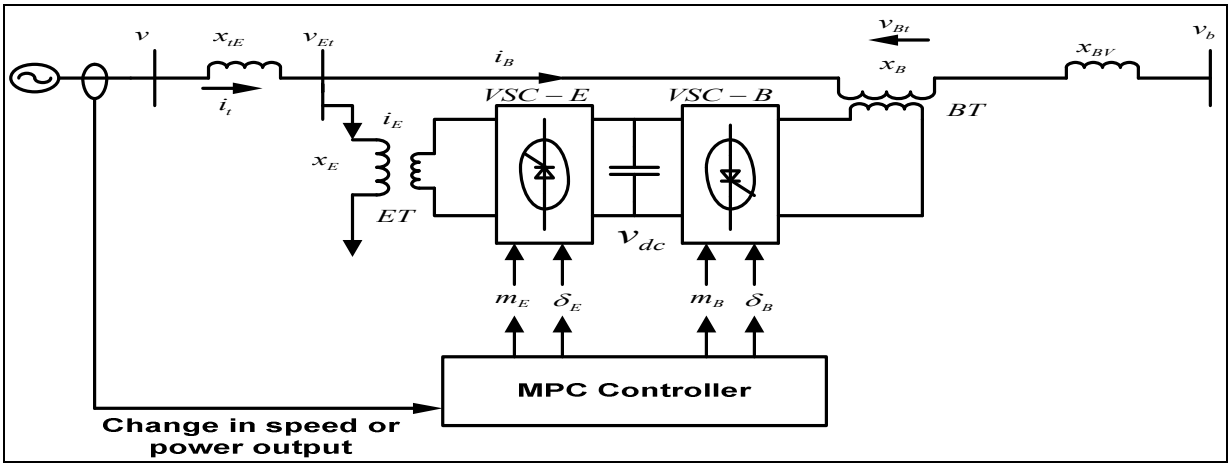

Figure 6.4: Circuital representation of UPFC connected SMIB system controlled with MPC (modification of Fig. 3.4)

6.4 Control of MPC

The MPC design problem is handled by the MPC toolbox available in 'Matlab'.

A Model Predictive Control Toolbox design requires a plant model, which defines the mathematical relationship between the plant inputs and outputs as shown in Figure 6.5. The controller uses it to predict plant behavior. The toolbox software requires the model to be linear, time invariant (LTI).

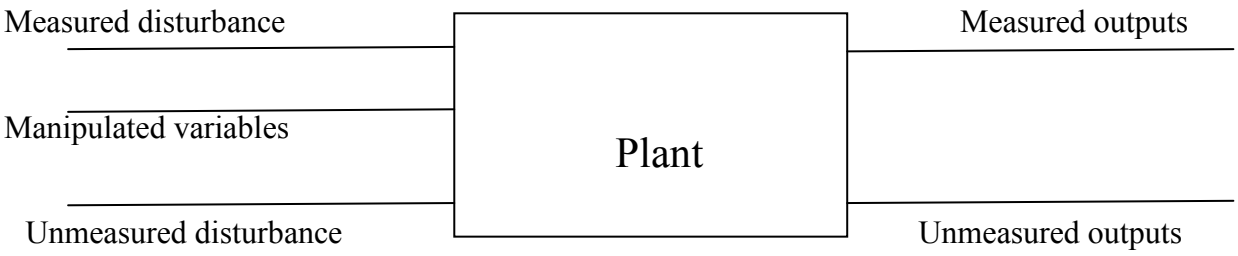

Fig 6.5: Plant with Input and Output Signals

The **plant inputs** are the independent variables affecting the plant. As shown in the previous figure, there are three types:

Measured disturbances: The controller can't adjust them, but uses them for feedforward compensation.

Manipulated variables: The controller adjusts these in order to achieve its goals.

Unmeasured disturbances: These are independent inputs of which the controller has no direct knowledge, and for which it must compensate.

The **plant outputs** are the dependent variables (outcomes) one wishes to control or monitor. As shown in figure 6.5, there are two types:

Measured outputs: The controller uses these to estimate unmeasured quantities and as feedback on the success of its adjustments.

Unmeasured outputs: The controller estimates these based on available measurements and the plant model. The controller can also hold unmeasured outputs at setpoints or within constraint boundaries.

The design and performance evaluation of the MPC is conducted based on changing the following parameters (Figure 6.6):

- Model and Horizons
- Constraint
- Weight Tuning
- Estimation

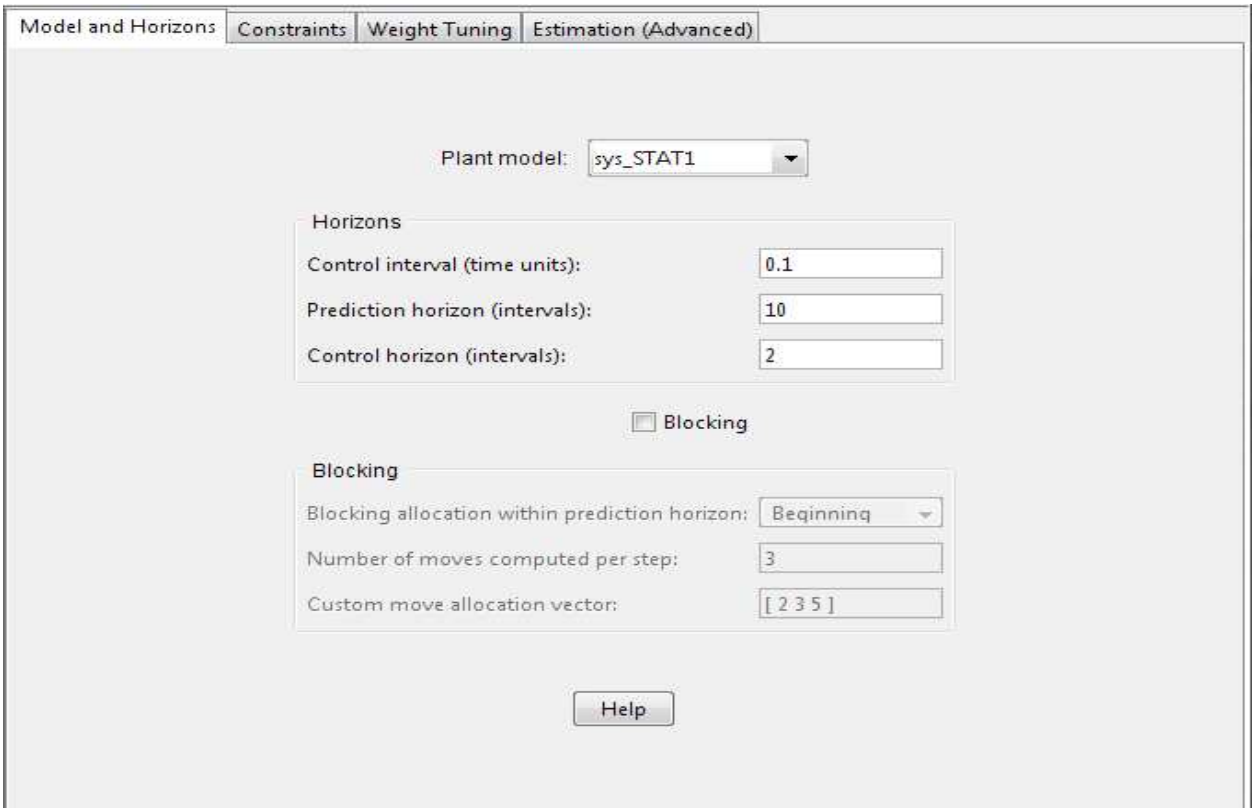

Figure 6.6: MPC controllers

From Fig.6.6 we can see that the model and horizons tab has parameters:

- Control interval (time units),
- Prediction horizon (intervals)
- Control horizon (intervals).

Prediction horizon (Hp) is the number of steps for which the controller will estimate the output of the system say (5,10,20,30,40,50 intervals, etc) also known as output horizon. **Control horizon** (Hc) is the number of steps (2, 4, 6, 8, etc) for which the controller will create future control action to fulfill all the requirements. **Control interval** (sampling period in sec) is the interval (0.1, 0.3, 0.7, 1, etc) separating successive sampling instants.

It is better to set the **constraints** for all manipulated variables, but it's unwise to enter constraints on outputs unless they are an essential aspect of the application. The “Max down rate” should be nonpositive (or blank). It limits the amount a manipulated variable can decrease in a single control interval. Similarly, the “Max up rate” should be nonnegative. It limits the increasing rate. Leave both unconstrained (i.e., blank).

The **weights** specify trade-offs in the controller design. First consider the Output weights. The controller will try to minimize the deviation of each output from its setpoint or reference value. For each sampling instant in the prediction horizon, the controller multiplies predicted deviations for each output by the output's weight, squares the result, and sums over all sampling instants and all outputs. One of the controller's objectives is to minimize this sum, i.e., to provide good setpoint tracking.

The **Estimation** tab allows to adjust the controller's response to unmeasured disturbances.

6.5 Response of UPFC connected SMIB system for MPC

A disturbance of pulse type signal is given in the system’s ΔP_e. Disturbance type is exactly similar to that of the disturbance which has been given in the system earlier while operating with PSS and PI controller. Response of MPC on proposed model is observed for 5 different states $\Delta\delta$, $\Delta\omega$, $\Delta E'_q$, ΔE_{fd} and ΔP_e. Individual effects of 4 different control signals m_E, δ_E, m_B and δ_B on system states are observed first in figure (6.5.1-6.5.4)

6.5.1 Response for control signal m_E only

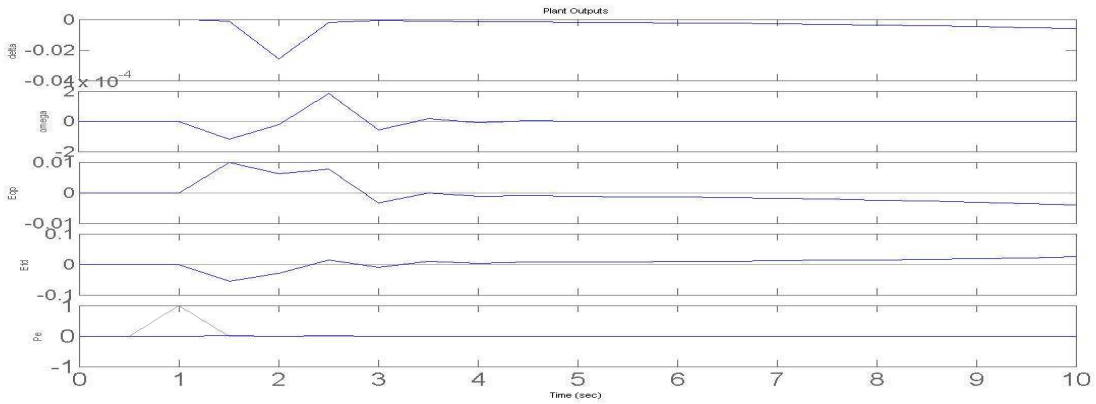

Fig 6.7: Responses of MPC connected SMIB system for control signal m_E for states (i) Δδ, (ii) Δω, (iii) $\Delta E'_q$,and (iv) ΔE_{fd}

It has been found that (Fig 6.7) control signal m_E can stable only the state Δω at a time of 4.8 seconds which has the maximum peak of 1.9pu. State Δδ reaches at $-0.03X10^{-4}$pu peak, $\Delta E'_q$ at 0.01pu peak and ΔE_{fd} at -0.05pu peak. But none of these states become complete stable here while controlling with m_E.

6.5.2 Response for control signal m_B only

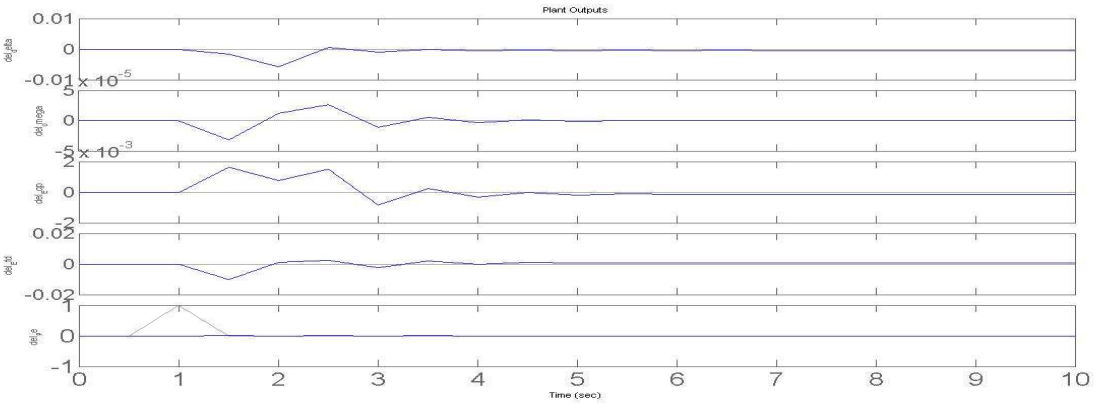

Fig 6.8: Responses of MPC connected SMIB system for control signal m_B for states (i) Δδ, (ii) Δω, (iii) $\Delta E'_q$,and (iv) ΔE_{fd}

It has been found that (Fig 6.8) control signal m_B can stable all the states successfully. State Δω

becomes stable at a time of 5.3 seconds which has the maximum peak of $2.5X10^{-5}$pu. State $\Delta\delta$ reaches upto -0.006 pu peak and has a settling time of 6.8seconds. $\Delta E'_q$ reaches at 1.85pu peak and has a settling time of 5.8seconds. ΔE_{fd} reaches at -0.015pu peak and has a settling time of 4.8

6.5.3 Response for control signal δ_E only

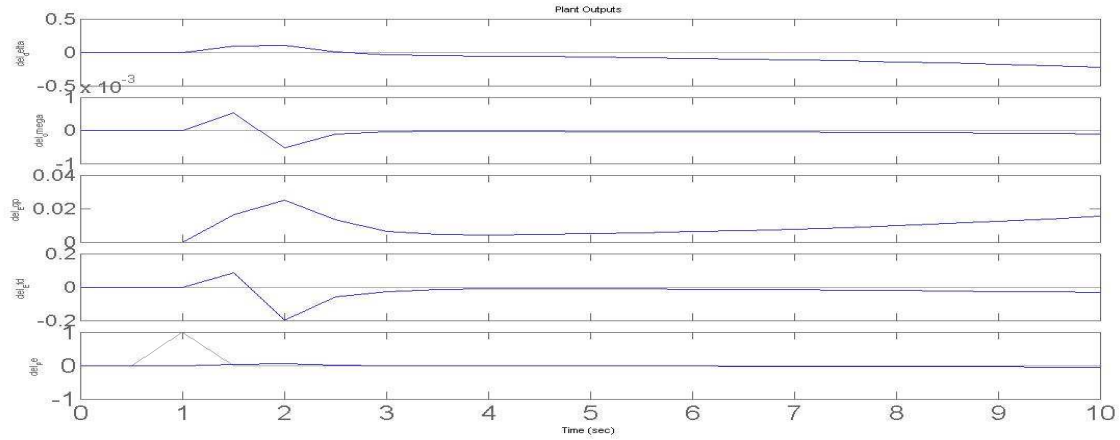

Fig 6.9: Responses of MPC connected SMIB system for control signal δ_E for states (i) $\Delta\delta$, (ii) $\Delta\omega$, (iii) $\Delta E'_{q,}$and (iv) ΔE_{fd}

Among the single input responses, response of control signal δ_E is the worst. Only the state $\Delta\omega$ become stable with a settling time of 2.9 seconds and a maximum peak of 0.7pu. MPC can not bring stability in other 3 states.

6.5.4 Response for control signal δ_B only

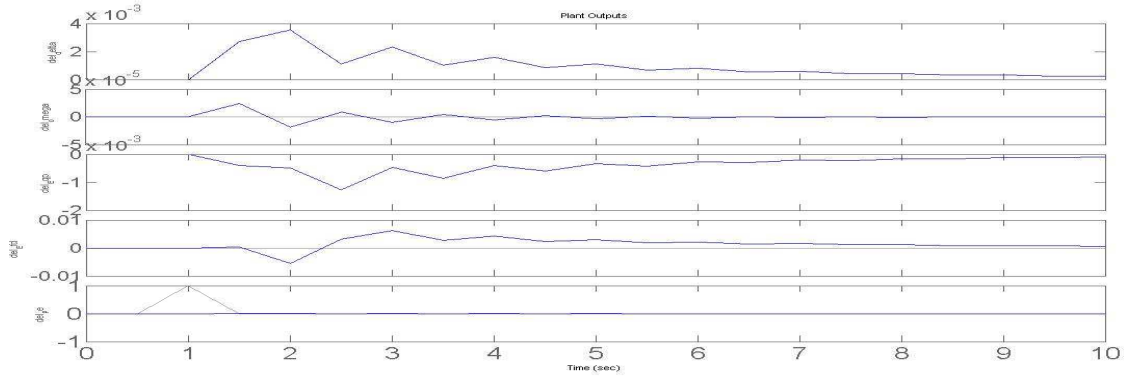

Fig 6.10: Responses of MPC connected SMIB system for control signal δ_B for states (i) $\Delta\delta$, (ii) $\Delta\omega$, (iii) $\Delta E'_{q,}$and (iv) ΔE_{fd}

It has been found from the Fig. 6.10 that control signal δ_B makes state $\Delta\omega$ and ΔE_{fd} stable but takes a very long time for that. Overall the response is not good.

An exceptional and effective feature of MPC is the ability to provide support to the MIMO plants. Most MPC toolbox applications involve plants having multiple inputs and outputs. Here, combination of different control signals of UPFC is now applied as input to the plant to observe the responses on different states.

6.5.5 Response for control signals m_B & δ_B together

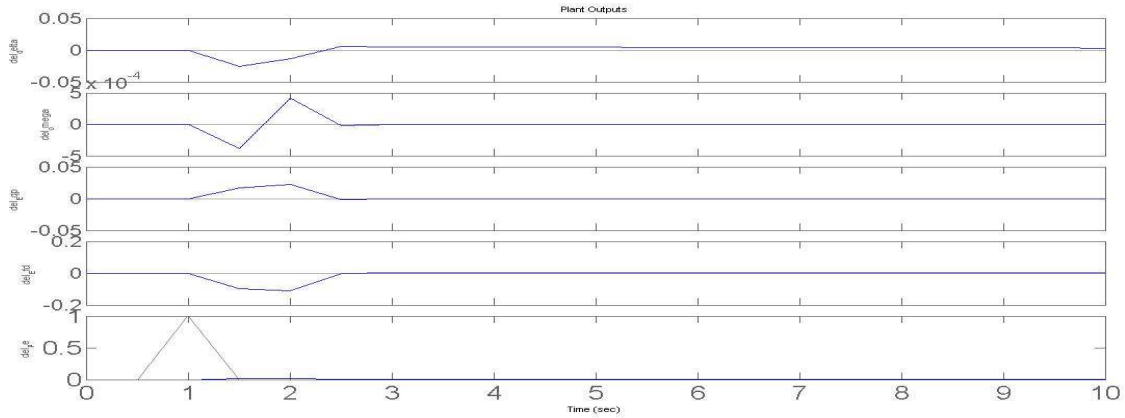

Fig 6.11: Responses of MPC connected SMIB system for control signal m_B & δ_B for states (i) $\Delta\delta$, (ii) $\Delta\omega$, (iii) $\Delta E'_q$ and (iv) ΔE_{fd}

Applying multiple inputs has provided a very satisfactory response here. Combination of m_B & δ_B brings stability (Fig 6.11) in all the four states at a very short time of 2.7 seconds. Maximum peak values are also reasonable.

6.5.6 Response for control signals m_E & δ_E together

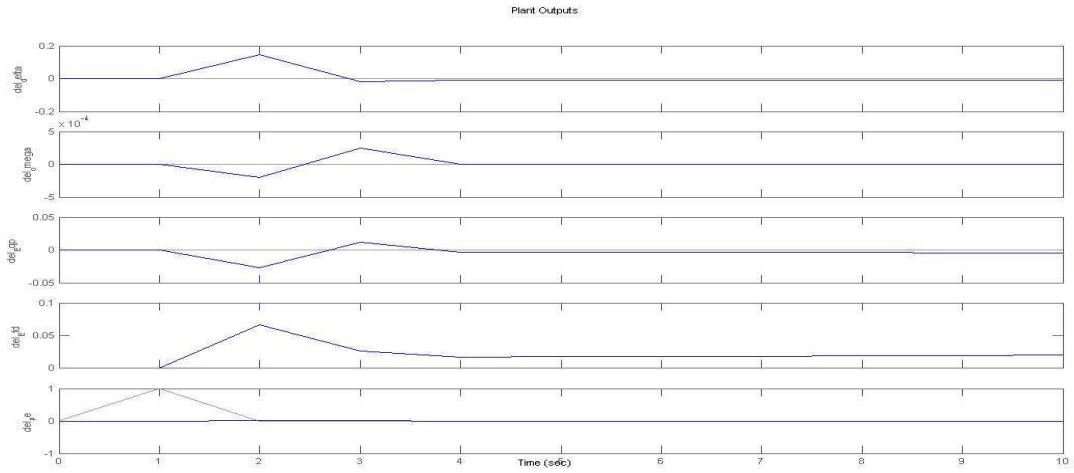

Fig 6.12: Responses of MPC connected SMIB system for control signal m_E & δ_E for states (i) $\Delta\delta$, (ii) $\Delta\omega$, (iii) $\Delta E'_q$,and (iv) ΔE_{fd}

It has been found that (Fig 6.12) the combination of m_E & δ_E also can stable all the states. State $\Delta\delta$ needs 3 seconds to settle, other 3 states takes around 4 seconds to be stable.

6.5.7 Response for control signals m_E & m_B together

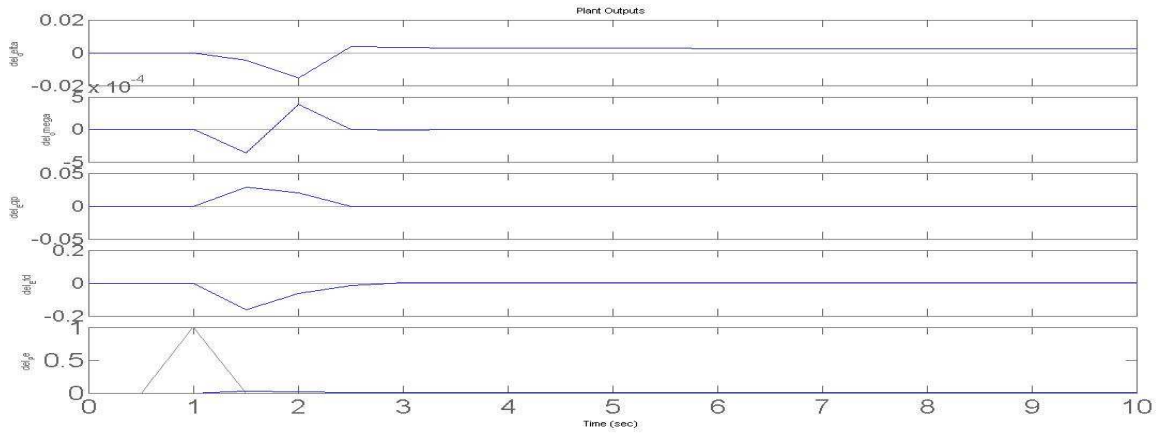

Fig 6.13: Responses of MPC connected SMIB system for control signal m_B & m_E for states (i) $\Delta\delta$, (ii) $\Delta\omega$, (iii) $\Delta E'_q$,and (iv) ΔE_{fd}

It has been seen that (Fig 6.13) the combination of m_E & m_B also can stable all the states. State $\Delta\delta$, $\Delta\omega$ and $\Delta E'_q$ needs a very short time (2.5 seconds) to be stable, where state ΔE_{fd} takes around 2.8 seconds to be stable.

6.5.8 Response for control signals δ_E & δ_B together

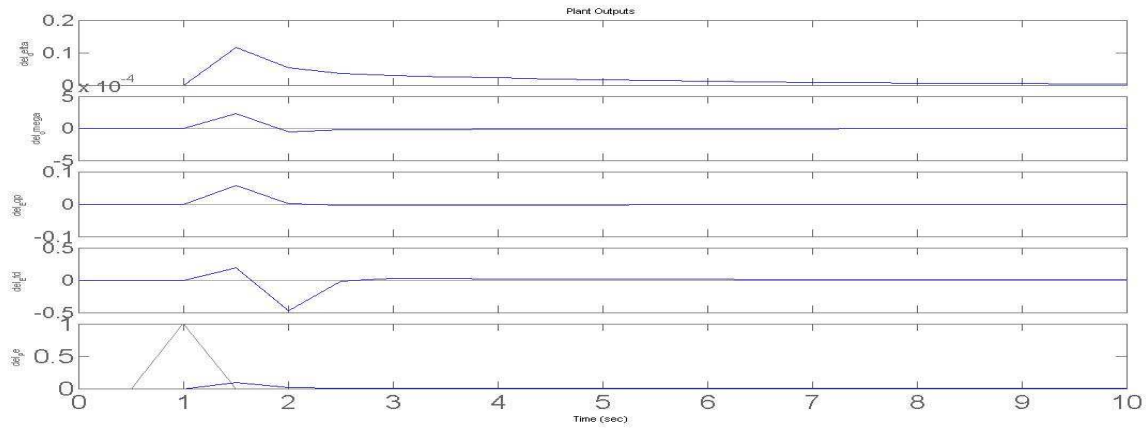

Fig6.14: Responses of MPC connected SMIB system for control signal δ_B & δ_E for states (i) $\Delta\delta$, (ii) $\Delta\omega$, (iii) $\Delta E'_q$, and (iv) ΔE_{fd}

States $\Delta\omega$ and $\Delta E'_q$ shows that (Fig 6.14) the best response while operating with the combination of δ_B & δ_E. They have a settling time of only 2 seconds. ΔE_{fd} needs 2.5 seconds to be stable. But, $\Delta\delta$ needs a long time to settle down (8 seconds).

6.5.9 Response for control signals δ_E & m_B together

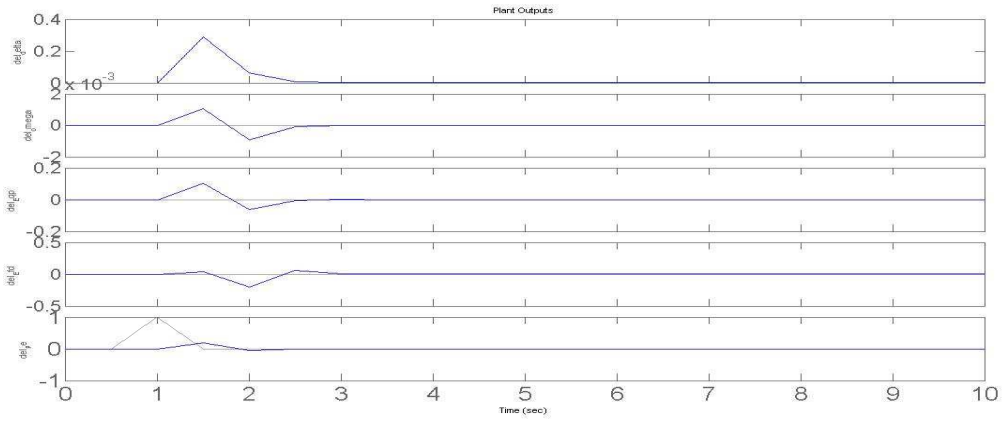

Fig6.15: Responses of MPC connected SMIB system for control signal m_B & δ_E for states (i) $\Delta\delta$, (ii) $\Delta\omega$, (iii) $\Delta E'_q$, and (iv) ΔE_{fd}

It has been found that (Fig 6.15) combination of m_B & δ_E makes the entire four stable within a very short time of around 2.5seconds. Response for this combination is very satisfactory and best among the combinations of double input signals.

6.5.10 Response for all four control signals together

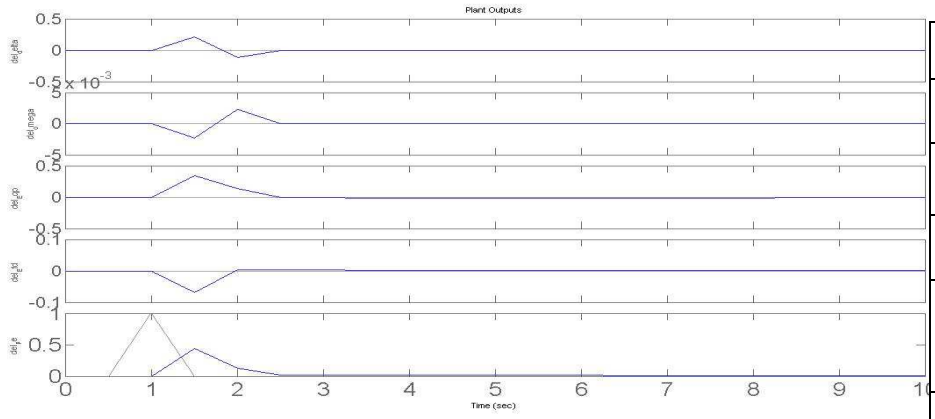

Case 1	
Control interval	0.5
Prediction horizon	10
Control horizon	2
Disturbance period(sec)	1
Dist.Amplitude(pu)	1

Fig6.16: Responses of MPC connected SMIB system for all four control signals for states (i) $\Delta\delta$, (ii) $\Delta\omega$, (iii) $\Delta E'_q$ and (iv) ΔE_{fd}

It has been found that (Fig 6.16) the best response among all the observations are found when the plant is given four control signals at a time. State ΔE_{fd} become stable at 2 seconds and the other three states are also been stable at a very short time of 2.5 seconds.

This response has been chosen here as case 1 and changes in different parameters from controller toolbox are made here to observe the respective changes in responses.

6.6 Effect of changing control parameters:

Control interval, prediction horizon and control horizon are considered as 1 second, 10 intervals and 2 intervals respectively as base case 1. Effects for the entire four control signals together (fig 6.16, case 01) are now observed for changing the different parameters of three controllers.

6.6.1 Effect of changing control interval (time units)

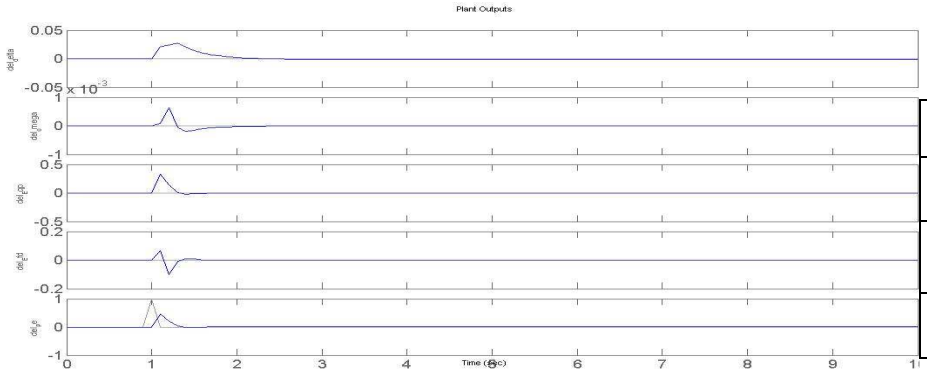

Case 2	
Control interval	0.1
Prediction horizon	10
Control horizon	2

Figure 6.17: Plant output for case 2

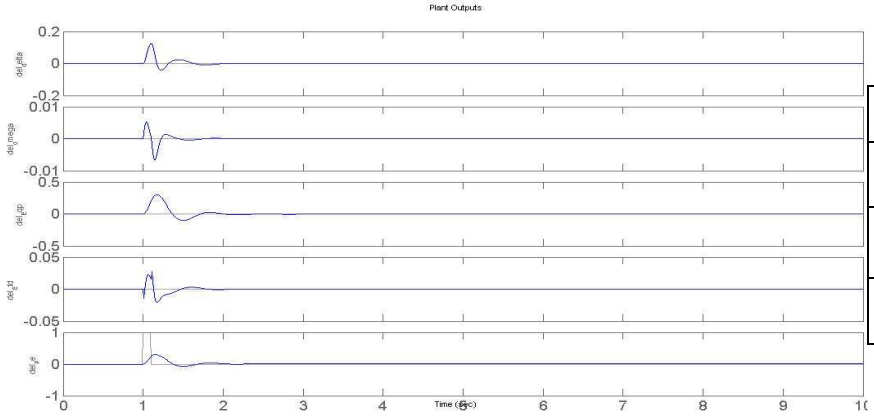

Case 3	
Control interval	0.01
Prediction horizon	10
Control horizon	2

Figure 6.18: Plant output for case 3

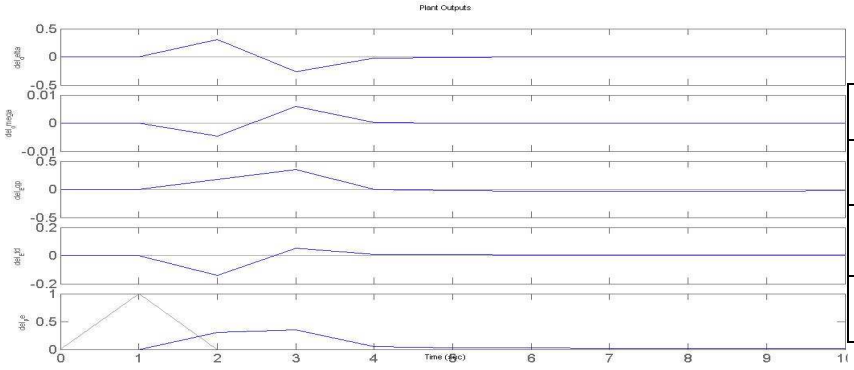

Case 4	
Control interval	1
Prediction horizon	10
Control horizon	2

Figure 6.19: Plant output for case 4

Observing Fig. (6.17-6.19) and comparing with fig. 6.16 (case 01), it is seen that the increase of control interval hampers the system response (case 4) while reducing of control interval improves response (case 2,3) providing the better settling time.

6.6.2 Effect of changing prediction horizon (time units):

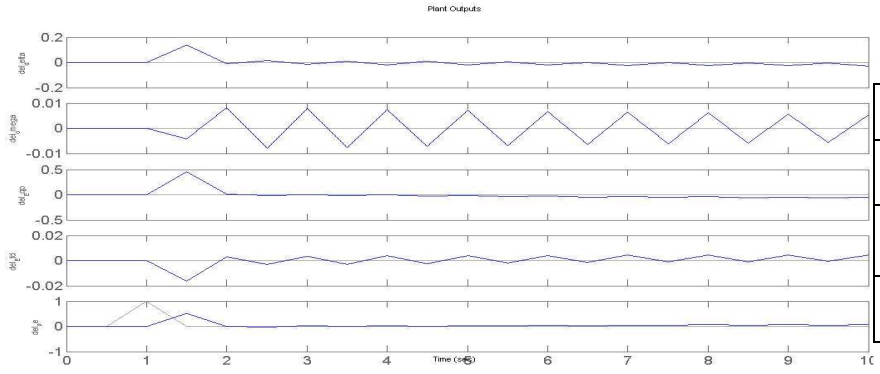

Case 5	
Control interval	0.5
Prediction horizon	2
Control horizon	2

Figure 6.20: Plant output for case 5

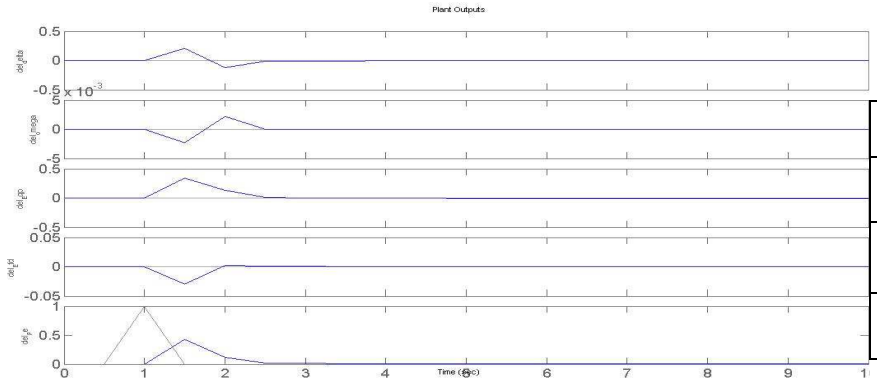

Case 6	
Control interval	.5
Prediction horizon	4
Control horizon	2

Figure 6.21: Plant output for case 6

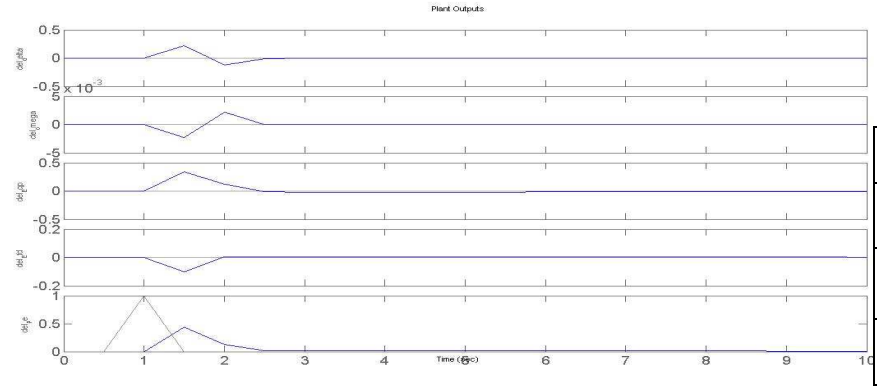

Case 7	
Control interval	.5
Prediction horizon	15
Control horizon	2

Figure 6.22: Plant output for case 7

Observing Fig. (6.20-6.22) and comparing with fig. 6.16 (case 01), it has been observed that the increase or decrease of prediction horizon by a small margin do not hamper the system response (case 6,7) while reducing of prediction horizon by a large margin hampers system response a lot (case 5).

6.6.3 Effect of changing control horizon (time units):

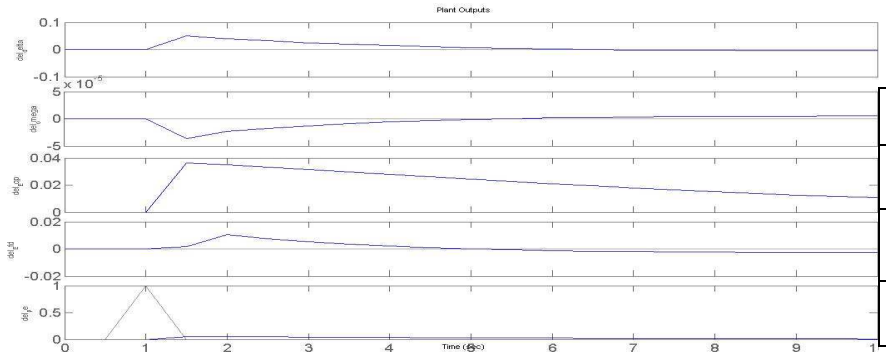

Case 8	
Control interval	0.5
Prediction horizon	10
Control horizon	1

Figure 6.23: Plant output for case 8

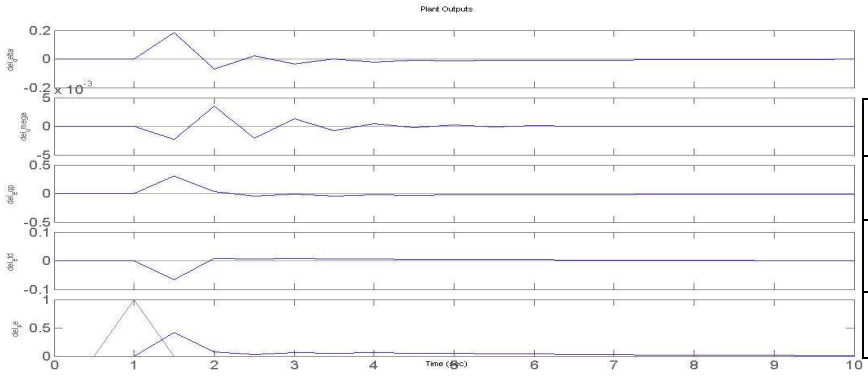

Case 9	
Control interval	0.5
Prediction horizon	10
Control horizon	4

Figure 6.24: Plant output for case 9

Observing Fig. (6.23-6.24) and comparing with fig. 6.16 (case 01), it has been observed that the decrease of control horizon hamper system response badly (case 8) while increasing of prediction horizon hampers system response as well (case 9) but not that much like case 8.

6.6.4 Effect of changing disturbance duration (period):

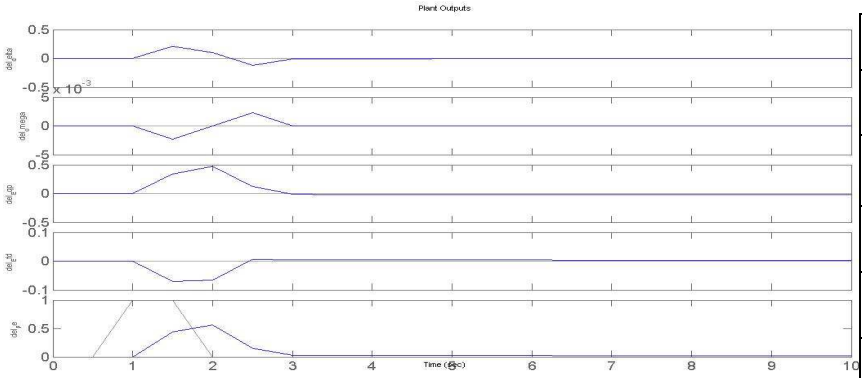

Case 10	
Control interval	0.5
Prediction horizon	10
Control horizon	2
Disturbance period	1
Dist. Amplitude	1

Figure 6.25: Plant output for case 10

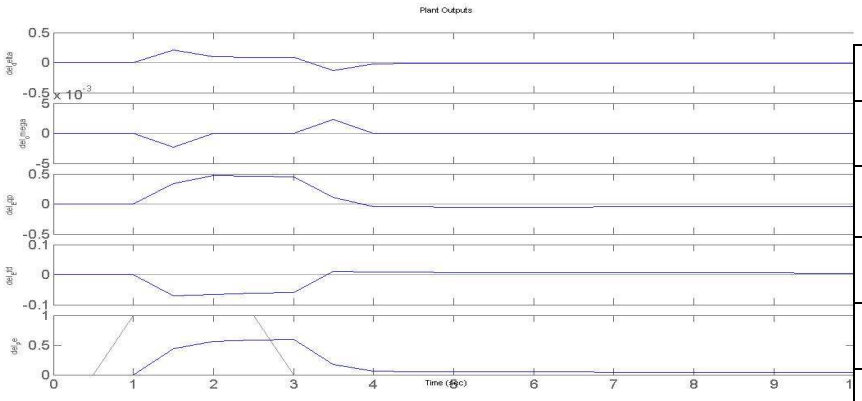

Case 11	
Control interval	0.5
Prediction horizon	10
Control horizon	2
Disturbance period	2
Dist. Amplitude	1

Figure 6.26: Plant output for case 11

It has been seen from Fig. 6.25 & 6.26 that the increase in disturbance duration increases the settling time accordingly. Comparison of case 10 & 11 with case 01 clearly shows the increase of rise time.

6.6.5 Effect of changing disturbance amplitude (size):

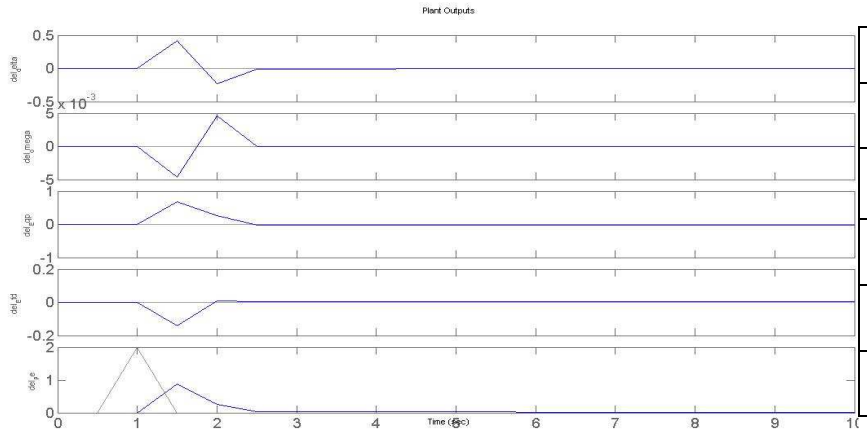

Case 12	
Control interval	0.5
Prediction horizon	10
Control horizon	2
Disturbance period	1
Dist. Amplitude	2

Figure 6.27: Plant output for case 12

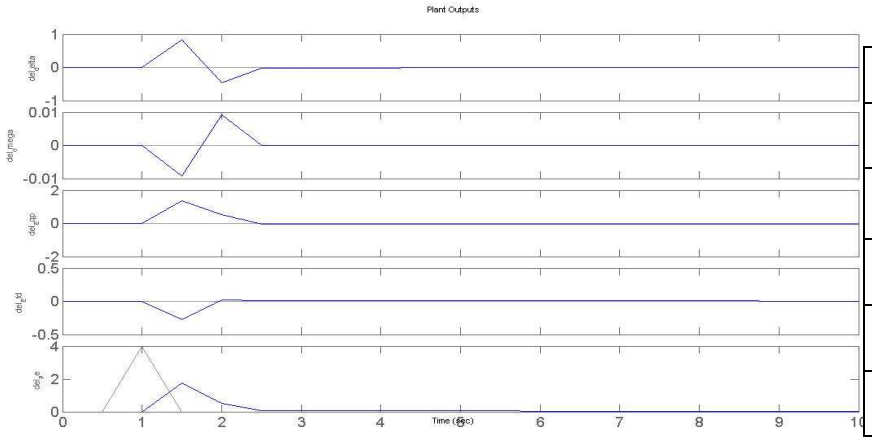

Case 13	
Control interval	0.5
Prediction horizon	10
Control horizon	2
Disturbance period	1
Dist. Amplitude	4

Figure 6.28: Plant output for case 13

It has been seen from Fig. 6.27 & 6.28 that the increase in disturbance amplitude do not effect the settling time but increase the response amplitude accordingly. Comparison of case 12 & 13 with case 1 clearly shows the increase of maximum peak values of the responses.

Observing the responses (from chapter 4 & 6), the total outcomes can be summarized in a single table from which comparison can be made easily between the impacts of three controllers (PSS, PI and MPC).

PSS		***PSS+ PI***				***MPC***			
i/p signal	**Stability**	**i/p signal**	**Stability**	**Settling time(sec)**	**Oscillati--on peak(pu)**	**i/p signal**	**Stability**	**Settling time(sec)**	**Oscillati--on peak(pu)**
m_E	Unstable	m_E	Unstable			m_E	Stable	4.5	$2\ X10^{-4}$
m_B	Unstable	m_B	Stable	5	0.011	m_B	Stable	4.8	$2.5X10^{-5}$
δ_E	Unstable	δ_E	Stable	5.5	0.013	δ_E	Stable	2.9	$0.5X10^{-5}$
δ_B	Unstable	δ_B	Unstable			δ_B	Stable	6.5	$2X10^{-5}$
						m_E& m_B	Stable	2.5	$4.5X10^{-4}$
						m_E & δ_E	Stable	4	$2.5X10^{-4}$
						m_B & δ_B	Stable	2.8	$4.5X10^{-4}$
						δ_E & δ_B	Stable	2	$2.5X10^{-4}$
						m_B & δ_E	Stable	2.5	$1X10^{-3}$
						All 4signals	Stable	2.5	$1X10^{-3}$

Table 6.1: Comparison of system responses on state $\Delta\omega$ for three different controllers

So, it has been seen from the above table that the system response has been improved significantly while operating the plant with MPC in the place of PSS and PI. PSS can't bring stability in state $\Delta\omega$ with any of the control signal, where PI controller is able to do that for two control signals with reasonable rise time and oscillation peak. Finally, use of MPC in plant model makes the state stable for all the control signals. Ability of MPC to work with more than one number of control signals has made it more versatile and effective. Impact of system response for multiple inputs has been found more satisfactory. Settling time and maximum peak value has to be significantly better than that of PI controller.

Chapter 7

Conclusions and Future Work

7.1 Summary

The dynamic behavior of a SMIB system installed with UPFC at the middle of the transmission line while controlling with MPC toolbox has been investigated in this thesis. Nonlinear dynamic model for the power system with UPFC is derived and a linearized model is obtained from that. The UPFC connected with SMIB is modeled by five state equations.

Oscillations created by a pulse type disturbance is then tried to be controlled by different controllers. Power system stabilizer (PSS) is connected first with the plant to observe the response but not a satisfied kind of performance was found there. PSS was unable to stable any one of the states ($\Delta\delta$, $\Delta\omega$, $\Delta E'_{q,}$and ΔE_{fd}) operating with any one of the control signals (m_E, m_B, δ_E, and δ_B). So, Proportional Integral (PI) controller was added then with the plant along with PSS to observe the system responses. Better performance was found here than the first one. Control signal m_B and δ_E brings stability different states with reasonable settling time and peak value. Responses for PSS and PI are then showed for two other loading conditions (light and heavy). Eigen values are also found to check the stability. The result for Eigen value analysis and response plots were found same.

The use of MPC for UPFC is shown then for the SMIB system. Responses were observed for single inputs as well as multiple inputs. The performance of MPC for SMIB system is tested by varying the different control parameters of MPC.

7.2 Contribution

Significantly improved result was found for every case than that of PSS and PI controller. Overview of all the results is shown in a table (table 6.1) for a particular state, $\Delta\boldsymbol{\omega}$. It has been found that variation of control interval up to a certain extent gives satisfactory result. Decrease of control interval improves the system response as it increases the number of control moves. And, increase of control interval decreases the number of control moves, so the response become worse. The variation of prediction horizon has little impact on the controller performance unless

it has been made very large. The controller designed was tested for a number of disturbance conditions as well. The MPC design has been found to be very effective for a range of operating conditions of the power system.

7.3 Conclusion

Model predictive controller (MPC) with a combination with unified power flow controller (UPFC) has been shown in this thesis as an effective solution of power system stability. Study is made with a system having a single machine as source and an infinite bus as load. Ability of MPC to work with MIMO plants and to work in real time mode has made it an effective choice for system damping. Some recommendations are given in the next section which are needed to be studied.

7.4 Recommendations for Future Work

In the following, some recommendations are given for future research in the area.

- Further research is needed to evaluate the impact of all the control parameters of MPC more accurately.
- System responses for applying the combinations of three control signals of UPFC at a time can be investigated.
- The research has been done here for a model containing a single machine. So, the effect of UPFC on multi-machine system stability needs investigation while controlling with MPC. The locations of the UPFC devices in a multi-machine system require careful study.
- In this study of UPFC connected SMIB, UPFC is located at the middle of the transmission line. The impact of the location of the UPFC other than middle of the transmission line on the dynamic performance can be also studied.

References

[1] Padiyar, P K “Power system stability and control” EPRI Power system series,1994.

[2] Anderson, PM - Fouad, A A “Power system control and stability” Iowa state university press, 1980.

[3] Hingorani, N G - Gyugyi, L "Understanding FACTS: concepts And Technology of Flexible AC Transmission Systems” IEEE press, 2000.

[4] Hingorani, N G "Power Electronics in Electric Utilities: Role of power electronics in future power systems" Proceedings of the IEEE, vol. 76, pp. 481, 1988.

[5] Edwards et al, C W "Advanced Static Var Generator Employing GTO Thyristors" IEEE, PES winter Power Meeting, Paper No. 38wm109-1, 1988.

[6] Ajami, A – Asadzadeh, H “Damping of power system oscillations using UPFC based multipoint tuning AIPSO-SA algorithm” Gazi University Journal of Science, 24(4):791-804, 2011.

[7] Tambey, N – Kothari, M L “Damping of power system oscillations with unified power flow controller (UPFC)” IEE Proc.-Gener. Transm. Distrib., Vol. 150, No. 2, March 2003.

[8] Rahim, A H M A - Al-Baiyat, S A “On-line identification and control through series converter voltage of a unified power flow controller” The Mediterranean Journal of Measurement and Control, Vol. 2, No. 3, 2006.

[9] Kamath, A K – Singh, N M – Wagh, S R "Transient Stability Enhancment of Power System Using MPC Based TCSC Controller" Bhil School of Electrical ,Electronic and Computer Engineering,University of Westren Australia, 2010.

[10] Orukpe, P E – Jaimuokha, I "Basics of Model Predictive Control" ICM, EEE-CAP,April 14, 2005. Imperial College,London.

[11] Nabavi Niaki, A - Iravani, M R "Steady-state and dynamic models of unified power flow controller (UPFC) for power system studies" IEEE Trans. Power Systems, vol. 11, no. 4,pp. 1937–1943, November 1996.

[12] Wang, H F "Damping function of unified power flow controller" IEE Proc. Gen. Trans. And Distrib, vol. 146, no. 1, pp. 81–87, 1999.

[13] Wang, H F "Application of modeling UPFC into multi-machine power systems" IEE Proc.Gen. Trans. and Distrib, vol. 146, no. 3, pp. 306–312, 1999.

[14] Heffron, W G - Phillips, R A "Effect of modern amplidyne voltage regulators on underexcited operation of large turbine generator" AIEE Trans. Power Apparatus and Systems, pp. 692–697, August 1952.

[15] Zhengyu, H - Yinxin, N - Shen, C M - Wu, F F - Shousun, C – Baolin Z "Application of unified power flow controller in interconnected power systems—modeling, interface, control strategy and case study," IEEE Trans. Power Systems, vol. 15, no. 2, pp. 817–824, May 2000.

[16] Dash, P K - Mishra, S – Panda G "A radial basis function neural network controller for UPFC" IEEE Trans. Power Systems, vol. 15, no. 4, pp. 1293–1299, November 2000.

[17] Vilathgamuwa, M – Zhu, X – Choi, S S "A robust control method to improve the performance of a unified power flow controller" Electrical Power Systems Research 55 (2000), 103-111.

[18] Pal, B C "Robust damping of interarea oscillations with unified power flow controller" IEE Proc. on Generation, Transmission and Distribution 149 No. 6 (2002), 733-738.

[19] Kazemi, A – Vakili, M - Sohrforouzani "Power system damping controlled facts devices" Electrical Power and Energy Systems 28 (2006), 349-357.

[20] Dash, P K – Mishra, S – Panda, G "Damping multimodal power system oscillation using hybrid fuzzy controller for series connected FACTS devices" IEEE Transaction on Power Systems 15 No. 4 (2000), 1360-1366.

[21] Limyingcharone, S – Annakkage, U D – Pahalawaththa, N C "Fuzzy logic based unified power flow controllers for transient stability improvement" IEE Proc. On Generation, Transmission and Distribution 145 No. 3 (1998), 225-232.

[22] Chen, X R – Pahalawaththa, N C – Annakkage, U D – Cumble, C S "Design of decentralized output feedback TCSC damping controllers by using simulated annealing" IEE Proc. on Generation, Transmission and Distribution 145 No. 5 (1998), 553-558.

[23] Pourbeik, P – Gibbard, M J "Simultaneous coordination of power-system stabilizers and FACTS device stabilizers in a multi-machine power system for enhancing dynamic performance" IEEE Transaction on Power Systems 13 No. 2 (1998), 473-479.

[24] Cai, L J – Erlich, I "Simultaneous coordinated tuning of PSS and FACTS damping controllers in large power systems" IEEE Transaction on Power Systems 20 No. 1 (2005), 294-300.

[25] Abdel-Magid, Y L – Abido, M A "Robust coordinated design of excitation and TCSC-based stabilizers using genetic algorithms" Electrical Power Systems Research 69 (2004), 129-141.

[26] Lei, X – Lerch, E N – Povh, D "Optimization and coordination of damping controls for improving system dynamic performance" IEEE Transaction on Power Systems 16 No. 3 (2001), 473-480.

[27] Stagg, G W - Abaid, A H E L "Computer methods in power systems (New York Hills), 1968.

[28] Kimbark, E W " Power system stability" , vol. 1, John Wiley and Sons Inc., New York, 1948.

[29] Yu, Y N "Electric power system dynamics", Academic press 1983.

[30] Lerch, E - Porh D - Xu, L "Advanced SVC control for damping power system oscillations", 1991.

[31] Mithulananthan, N - Canizares, C.A – Reeve, J - Rogers, G J "Comparison of PSS, SVC and STATCOM controllers for damping power system oscillations" IEEE transactions on power systems, vol. 18, no.2, pp 786-792, May 2003.

[32] Stankovic, A M - Stefanov, P C - Tadnor, G - Somajic, D J "Dissipativity as a unifying control design framework for suppression of low frequency oscillations in power systems" IEEE transaction on power system vol.14, no.1, pp 192-199 February 1999.

[33] Chen, J - Milanovic, J V - Huges, F M "Selection of auxiliary input signal and location of SVC for damping electro-mechanical oscillations" IEEE transactions on power system vol. pp 623-627 2001.

[34] Koterev, D N - Taylor, C W - Mittlestadt, W A "Model validation for August 10, 1996 WSCC system outage". IEEE transactions on power systems vol. 14, pp 967- 979, August 1999.

[35] Mithlananthan, N - Srivastva, S C "Investigation of voltage collapse in Srilanka's power system network" In proc EMPD Singapore, pp 47-52, March 1995, IEEE catalog 98 EX 137.

[36] Demello, Molan, P J - Laskowski, T F - Udrill, J "Co-Ordinated application of stabilizers in multi-machine systems" IEEE transaction on PAS, vol. PAS -99, pp 892-902, 1980.

[37] Demello – Concordia C "Concepts of synchronous machine stability as affected by Excitation control" IEEE trans power APP and systems, vol. PAS 103, no 8, pp 1983-1989, 1984.

[38] Ahmed Mohamed Othman "Enhancing the Performance of Flexible AC Transmission Systems (FACTS) by Computational Intelligence" Aalto University publication series DOCTORAL DISSERTATIONS 55/2011.

[39] Acha, E - Fuerte, C R - Pe´rez, H A - Camacho, C A "FACTS Modelling and Simulation in Power Networks" John Wiley & Sons Ltd, West Sussex, ISBN 0-470-85271-2, pp. 9-12, 2004.

[40] Dong L Y – Zhang, L - Crow, M L "A new control strategy for the Unified Power Flow Controller" IEEE Power Engineering Society Winter Meeting, vol. 1, 2002, pp. 27-31.

[41] Padiyar K R - Rao, K U "Modeling and Control of Unified Power Flow Controller for Transient Stability" Electric Power Systems Research, 51, 1999, pp. 1-11.

[42] Schauder, C - Mehta, H "Vector Analysis and control of Advanced Static VAR Compensators" IEE Proceedings, Generation, Transmission and Distribution, vol. 140, no. 4, 1993.

[43] Limyingcharoen, S - Annakkage, U D - Pahalawaththa, N C "Fuzzy Logic Based Unified Power Flow Controllers for Transient Stability Improvement" IEE Proc. Genet. Transm. Distrib, Vol. 145, No. 3, 1998, pp. 225-232.

[44] Huang, Z – Ni, Y. Shen, C M - Wu, F F S - Chen, B Zhang "Application of Unified Power Flow Controller in interconnected power systems – modeling, interface, control strategy and case study" IEEE Power Engineering Society Summer Meeting, 1999.

[45] Papic, P - Zunko, D - Povh, M Weihold, "Basic control of Unified Power Flow Controller", IEEE Transaction on Power Systems, vol. 12, no. 4, 1997.

[46] Padiyar, K R - Kulkarni, A M "Control design and simulation of Unified Power flow Controller" IEEE Transactions on Power Delivery, vol. 13, no. 4, 1997, pp. 1348-1354.

[47] Pierre, D A “A Perspective on Adaptive Control of Power Systems” IEEE Trans. on Power Systems, PWRS-2(.5), 1987, pp 387-396.

[48] Ramakrishna, G - Malik, O P “Radial basis function identifier and pole-shifting controller for power system stabilizer application” IEEE Transactions on Energy Conversion, Vol. 19, No. 4 (2004), pp. 663-670.

[49] R. Segal, A. Sharma, M. L. Kothari, “A self-tuning power system stabilizer based on artificial neural network”, Electrical Power and Energy System Journal, 26 (2004), 423-430.

[50] R. You; H. J. Eghbali, M. H. Nehrir, “An on-line adaptive neuro-fuzzy power system stabilizer for multimachine systems”, IEEE PES General Meeting, 2003, vol. 4.

[51] A. Nabavi-Niaki and M. R. Iravani, “Steady-state and dynamic models of unified power flow controller (UPFC) for power system studies,” IEEE Trans. Power Systems, vol. 11, no. 4, pp. 1937–1943, November 1996.

[52] H. F. Wang, “Damping function of unified power flow controller,” IEE Proc. Gen. Trans. And Distrib, vol. 146, no. 1, pp. 81–87, 1999.

[53] H. F. Wang, “Application of modeling UPFC into multi-machine power systems,” IEE Proc. Gen. Trans. and Distrib, vol. 146, no. 3, pp. 306–312, 1999.

[54] Al-Awami A. T.- Abdel-Magid Y. L. - Abido M. A. : “Simultaneous Stabilization of Power System Using UPFC-Based Controllers”, Electric Power Components and Systems, 34:941–959, 2006.

[55] Qin S.J. and Badgwell T.A. “An overview of industrial model predictive control technology”, In F. Allg¨ower and A. Zheng, editors, Fifth International Conference on Chemical Process Control – CPC V, pages 232–256. American Institute of Chemical Engineers, 1996.

[56] Qin S.J. and Badgwell T.A. : “An overview of nonlinear model predictive control applications”, In F. Allg¨ower and A. Zheng, editors, “Nonlinear Predictive Control”, pages 369–393. Birkh¨auser, 2000.

[57] Ahmadzade B. – Shahgholian G. - Mogharrab Tehrani F. – Mahdavian M. : “Model Predictive control to improve power system oscillations of SMIB with Fuzzy logic controller”

[58] Eduardo F, Camacho and Carlos Bordons: “Model Predictive Control Advanced Textbooks in Control and Signal Processing”, Springer Publication, 1998.

[59] Allgower, F., Badgwell, T. A., Qin, S. J., Rawlings, J. B., & Wright, S. J. (1999). Nonlinear predictive control and moving horizon estimation—an introductory overview. In P. M. Frank (Ed.), Advances in control: highlights of ECC ’99. Berlin: Springer.

[60] Mayne, D. Q., Rawlings, J. B., Rao, C. V., & Scokaert, P. O. M. (2000). Constrained model predictive control: Stability and optimality. Automatica, 36, 789–814.

[61] Qin, S. J., & Badgwell, T. A. (1997). An overview of industrial model predictive control technology. In J. C. Kantor, C. E. Garcia, & B. Carnahan (Eds.), Chemical process control—V, Fifth international conference on chemical process control CACHE and AICHE, (pp.232–256).

[62] Young, R. E., Bartusiak, R. B., & Fontaine, R. B. (2001). Evolution of an industrial nonlinear model predictive controller. In Preprints: Chemical process control—CPC VI, Tucson, Arizona (pp. 399– 410). CACHE.

[63] Downs, J. J. (2001). Linking control strategy design and model predictive control. In Preprints: Chemical process control-6, assessment and new directions for research (CPC VI), Tuscon, AZ, January 2001 (pp. 411–422)

[64] Hillestad, M., & Andersen, K. S. (1994). Model predictive control for grade transitions of a polypropylene reactor. In Proceedings of the 4th European symposium on computer aided process engineering (ESCAPE 4), Dublin, March 1994.

[65] Ohshima, M., Ohno, H., & Hashimoto, I. (1995). Model predictive control: Experiences in the university-industry joint projects and statistics on MPC applications in Japan. International workshop on predictive and receding horizon control, Korea, October 1995.

[66] Richalet, J., Rault, A., Testud, J. L., & Papon, J. (1976). Algorithmic control of industrial processes. In Proceedings of the 4th IFAC symposium on identification and system parameter estimation. (pp. 1119–1167).

[67] Richalet, J., Rault, A., Testud, J. L., & Papon, J. (1978). Model predictive heuristic control: Applications to industrial processes. Automatica, 14, 413–428.

[68] Ford J.J. - Ledwich G. - Dong Z.Y :" Efficient and robust model predictive control for first swing transient stability of power systems using flexible AC transmission systems devices", IET Generation, Transmission & Distribution Received on 26th September 2007.

Appendices

Appendix A

The parameters used in Single Machine infinite bus (SMIB) power system modeling are:

Machine: Pt=1; Eb=1; Vt0=1; omega0=377; Td0p=.4; Tq0p=.1; H=4; freq=60,

Xe=0.25; Xq=1.7; Xd=1.8; Xdp=0.17; Xqp=0.23;

Exciter: TA=0.1; KA=10;
PSS: Upss=0; Kpss=4; Tw=1; T1=.1; T3=1; T2=1; T4=.1;

Appendix B

The parameters of the system used in optimization results of the UPFC are:

Generator: M = 8 MJ/MVA, T'_{d0} = 5.044 s, D = 0
X_q = 0.6 pu, X_d = 1.0 pu, X'_d = 0.3 pu
Excitation system: Ka = 100, Ta = 0.01 s
Transformers: X_T = 0.1 pu, X_E = 0.1 pu, X_B = 0.1 pu
Transmission line : X_L = 0.1 pu
Operating condition: P = 0.8 pu,Q=.1670pu , V_b = 1 pu, V_t = 1 pu
DC link parameter: V_{DC} = 2 pu, C_{DC} = 1.2 pu
UPFC parameter: m_E = 0.7667, m_B = 0.96, δ_E =68.113 deg, δ_B =41.118 deg

Appendix C

The table of constant values we have got in the linearized model of UPFC connected SMIB (Nominal loading):

K1	.2704		Kqd	.5591
K2	1.0830		Kqe	1.0826
K3	-2.4583		Kqde	.3334
K4	-.2138		Kqb	.1918

K5	-.0422		Kqdb	.2109
K6	.3437		Kvd	.2770
K7	.4798		Kve	.8381
K8	.4861		Kvde	-.0441
K9	.0783		Kvb	.1217
Kpd	.1275		Kvdb	.0440
Kpe	1.7560		Kce	.1973
Kpde	-.9711		Kcde	-1.3680
Kpb	.1771		Kcb	.0816
Kpbd	-.2546		Kcdb	1.0817

Appendix D

Table of information about different loading conditions:

Loading types»	**Nominal**	**Heavy**	**Light**
$\mathbf{P_e}$	.8	1.2	.2
$\mathbf{Q_e}$	.1670	.4	.01
$\mathbf{m_E}$	.7667	.7279	.7814
$\mathbf{m_B}$	.96	.985	.974
$\boldsymbol{\delta_E}$	68.113	56.640	89.113
$\boldsymbol{\delta_B}$	41.118	41.118	58.818
$\mathbf{i_d}$	.4730	.9485	.0336
$\mathbf{i_q}$	.6665	.8369	.1974